Journal of Statistical Physics, Vol. 41, Nos. 3/4, 1985

Static and Dynamic Properties of *XY* Systems with Extended Defects in Cubic Anisotropic Crystallines

Yoshitake Yamazaki,[1,2] Arno Holz,[2] Moyuru Ochiai,[3] and Yoshiichi Fukuda[4]

Received February 4, 1985; revision received June 15, 1985

Static and dynamic critical behavior of *XY* systems in cubic anisotropic crystallines, with extended defects (or quenched nonmagnetic impurities) strongly correlated along ε_d-dimensional space and randomly distributed in $d-\varepsilon_d$ dimensions, were studied. These extended defects make the systems coordinate anisotropic, resulting in unique critical behavior due to competition between the cubic anisotropy and the coordinate anisotropy. The systems were analyzed by an $\varepsilon^{1/2}$ ($\varepsilon \equiv 4-d$) type of expansion with double expansion parameters based on a renormalization-group (RG) approach. Critical exponents were calculated near the second-order phase transition point and the behavior of the first-order transition was evaluated near the tricritical point.

KEY WORDS: Phase transitions and critical phenomena; defects; random systems.

1. INTRODUCTION

Recently interest has been gathered in the statics and dynamics of various condensed media with structure defects.[1] For example, they are concerned with crystals with continuously distributed dislocations and disclinations, superfluids with quantized vertices, liquid crystals with disclinations, and so on. Further, as the same category we can regard amorphous matters, spin glasses, spin systems with frustations or with statistical defects, and so

[1] Department of Applied Physics, Tohoku University, Sendai, 980, Japan.
[2] Physik, Universität des Saarlandes, D66 Saarbrücken, West Germany.
[3] Department of Electronics, North Shore College, Atsugi, Kanagawa, 243, Japan.
[4] Physics, College of General Education, Tohoku University, Sendai, 980, Japan.

0022-4715/85/1100-0497$04.50/0

on. Efforts to classify defects in condensed media with the homotopy groups have been continued[2] but no general approach to the study of the statics and dynamics for them has yet been found. However, study of phase transitions and critical phenomena in simple model systems with structure defects, in particular in reduced spin systems, has been performed. In this paper attention has been focused on simplified spin models. Heretofore, pointlike defects have been treated as quenched random nonmagnetic impurities according to the following schemes: (1) the heuristic argument advanced by Harris[3]; (2) the renormalization-group (RG) approach to the $N(\geqslant 2)$-component systems, based on the $\varepsilon(\equiv 4-d)$ expansion ($d=$ dimensions of space), advanced by Grinstein and Luther,[4] Lubensky,[5] Aharony,[6] Yamazaki,[7] and others; (3) the RG approach to a single-component (Ising) system, based on the $\varepsilon^{1/2}$ expansion, advanced by Khmel'nitsukii[8] and Shalaev.[9] Extended linear or planar defects and randomly distributed pointlike defects in crystal lattices have been studied in quenched random impurity systems with extended impurities by Dorogovtsev,[10] Boyanovsky and Cardy,[11] Lawrie and Prudnikov,[12] and others. Their models were used for low densities of defects.

In the present paper we investigated the static and dynamic critical behavior of XY-spin systems in cubic anisotropic crystallines, with extended defects (or quenched nonmagnetic impurities) strongly correlated along ε_d-dimensional space and randomly distributed in $d-\varepsilon_d$ dimensions. It was assumed that defect density is lower than that of the critical percolation, and that cubic anisotropy does not disappear in low-density regimes. The extended defects make the lattice systems coordinate anisotropic, and unique critical behavior appeared as a consequence of the competition between cubic anisotropy and coordinate anisotropy. In addition to the features referred to above, the most striking new features of these systems are: (1) $\varepsilon^{1/2}$-type expansion can be applied to XY spin systems (previously this expansion method was applicable only for Ising systems) and (2) the first-order phase transition and the tricritical behavior can be more readily described.

In Section 2 the effective Hamiltonian and defect potential probability distribution of the systems is specified. In order to study static and dynamic properties of the systems within the frame of the Langevin equation using the replica method, the effective dynamic-replicated Hamiltonian and the generating functional of the vertex functions required for the study of the critical behavior of the systems was derived. In Section 3 the renormalization constants, applying the RG approach and the dimensional regularization scheme for systems with double expansion parameters $\{\varepsilon, \varepsilon_d\}$, were obtained. Using these renormalization constants the RG equations including their coefficient functions $\{\beta\}$, $\{\eta, \gamma, \zeta\}$ were deter-

mined in Section 4. According to the RG theory, the fixed points, their stability and the trajectories of flows in the interaction space, of the systems were evaluated. The static and dynamic critical exponents for perpendicular and parallel components of the systems were calculated on the flow trajectories of the second-order phase transition. In Section 5 the first-order phase transition was shown to appear near the marginal boundary of the thermodynamically stable region and its behavior, including the magnetization jump, temperature shift, etc., was evaluated at the transition point. Section 6 consists of conclusions.

2. HAMILTONIAN AND GENERATING FUNCTIONAL

For XY-spin systems in cubic-anisotropic crystallines with extended defects strongly correlated in ε_d dimensions and randomly distributed in $d-\varepsilon_d$ dimensions, the effective Hamiltonian is

$$\mathscr{H}(\varphi, V)=\int d^dx \left[\frac{1}{2}\sum_{\alpha=1}^{2}\{|\nabla_\perp \varphi_\alpha|^2+a_b^2|\nabla_\parallel \varphi_\alpha|^2+r_b\varphi_\alpha^2+V(x_\perp)\varphi_\alpha^2\}+\frac{\hat{u}_s}{4!}\left\{\sum_{\alpha=1}^{2}\varphi_\alpha^2\right\}^2+\frac{\hat{u}_c}{4!}\sum_{\alpha=1}^{2}\varphi_\alpha^4\right] \tag{2.1}$$

where $\hat{u}_s$ and $\hat{u}_c$ are the isotropic and cubic-anisotropic interactions, respectively. The order parameter (OP) of the spin fluctuations, $\varphi_\alpha(x, t)$ consists of two components ($\alpha=1, 2$), and r_b stands for the inverse magnetic susceptibility in the mean field (MF) theory. As the extended defects in ε_d dimensions (symbolized as the $\parallel$ component $x_\parallel$) made the space anisotropic, a coordinate-anisotropic constant a_b^2 was introduced. We consider the cases where the random defects distributed in $\tilde{d}$ ($\equiv d-\varepsilon_d$) dimensions (symbolized as the $\perp$ component $x_\perp$) can be regarded as an effect of random potentials; the atomic spacing $\ll$ the spin correlation length $\ll$ linear size between any pair defects, which are valid for defect concentrations well below the critical percolation concentration p_c. That is,

$$\mathscr{P}_v(V)=\mathscr{N}_v \exp\left[-(8\Delta)^{-1}\int d^{\tilde{d}}x_\perp\, V^2(x_\perp)\right] \tag{2.2}$$

where $\mathscr{N}_v$ is a normalization constant. This distribution generates only nontrivial correlation $\langle V(x_\perp)\, V(y_\perp)\rangle=\Delta\delta^{\tilde{d}}(x_\perp-y_\perp)$. Therefore, Δ stands for the amplitude of two-point correlation, i.e., it should be a positive constant which is proportional to both the defect concentration and random potential strength[13] as the zeroth-order contribution. In general, it is considered that the linear term in V shifts only the temperature term r_b and that

deviations from a Gaussian distribution are irrelevant and contribute only higher-order contributions (following arguments by Lubensky[5]). Anisotropy a_b^2 is induced by the extended defects. With the introduction of inhomogeneity in the quadratic term $[q_\perp^2 + a_b^2 q_\parallel^2 + r_b]|\varphi_\alpha(q, \omega)|^2$, the scaling dimensions in the diagram expansion are modified. Scaling each of the internal momenta (coordinates) $q_\perp(x_\perp)$ by unity and $q_\parallel(x_\parallel)$ by $a_b^{-1}(a_b)$, gives the dimensional relations

$$[a_b] = \left[\frac{\kappa_\perp}{\kappa_\parallel}\right], \qquad [\varphi^2] = [\kappa_\perp]^{d-2}[a_b]^{-\varepsilon_d}$$

$$[\hat{u}_s] = [\hat{u}_c] = [\kappa_\perp]^{4-d}[a_b]^{\varepsilon_d}, \qquad [\Delta] = [\kappa_\perp]^{4-d+\varepsilon_d} \tag{2.3a}$$

where [ ] denotes the dimensions in terms of the momentum units $\kappa_\perp$ and $\kappa_\parallel$. Thus the following expressions for the interactions were adopted:

$$\hat{u}_w \equiv a_b^{\varepsilon_d} u_w \qquad \text{for} \quad w = s, c \tag{2.4}$$

The static and dynamic properties of the systems are assumed to follow the Langevin equation[14]

$$\partial\varphi_\alpha(x, t)/\partial t = -\lambda_b\, \delta\mathscr{H}/\delta\varphi_\alpha(x, t) + \eta_\alpha(x, t) \qquad (\alpha = 1, 2) \tag{2.5}$$

where λ_b is the kinetic coefficient for the nonconserved systems. The Gaussian white-noise fields $\{\eta_\alpha(x, t)\}$ are defined by the probability functional

$$\mathscr{P}_\eta(\eta) = \mathscr{N}_\eta \exp\left[-(4\lambda_b)^{-1} \int d^d x\, dt \sum_{\alpha=1}^{2} \eta_\alpha^2(x, t)\right] \tag{2.6}$$

According to the method of Martin *et al.*,[15] Bausch *et al.*,[16] Dominicis *et al.*,[17] Yamazaki,[18] and Lawrie *et al.*,[12] this is reexpressed by introducing the response fields $\{\tilde{\varphi}_\alpha(x, t)\}$ and their source fields $\{\tilde{h}_\alpha(x, t)\}$ as

$$\mathscr{P}_\eta(\eta, \tilde{h}) = \mathscr{N}_\eta \int \mathscr{D}\tilde{\varphi} \exp\left[-\int d^d x\, dt \sum_{\alpha=1}^{2} \tilde{\varphi}_\alpha(\lambda_b^{-1}\tilde{\varphi}_\alpha + i\lambda_b^{-1}\eta_\alpha - \tilde{h}_\alpha)\right] \tag{2.7}$$

The generating functional for the connected correlation and response functions are

$$\mathscr{F}(\tilde{h}, h) = -\ln \mathscr{Z}(\tilde{h}, h)$$

$$\mathscr{Z}(\tilde{h}, h) \equiv \int \mathscr{D}\eta\, \mathscr{P}_\eta(\eta, \tilde{h}) \exp\left[\int d^d x\, dt \sum_{\alpha=1}^{2} h_\alpha(x, t)\, \varphi_\alpha(x, t)\right]$$

$$= \int \mathscr{D}\varphi \mathscr{D}\tilde{\varphi}\, \det|\delta\eta/\delta\tilde{\varphi}| \exp\left[\int d^d x\, dt \sum_{\alpha=1}^{2} (\tilde{h}_\alpha\tilde{\varphi}_\alpha + h_\alpha\varphi_\alpha) - \hat{\mathscr{H}}\right]$$

$$\hat{\mathscr{H}} \equiv \int d^d x\, dt[\tilde{\varphi}_\alpha\lambda_b^{-1}\tilde{\varphi}_\alpha + i\tilde{\varphi}_\alpha(\lambda_b^{-1}\,\partial\varphi_\alpha/\partial t + \delta\mathscr{H}/\delta\varphi_\alpha)] \tag{2.8}$$

where h_α denotes the source field for the OP field φ_α. The tadpole diagram of single response propagator loop in the perturbation expansions was neglected, and the Jacobian $|\delta\eta/\delta\tilde{\varphi}|$ dropped.

The correlation and response functions of the quenched random systems were calculated as the average of those generated over the random potentials. Using the replica method for this average procedure ($\langle\ \rangle_{\mathrm{RA}}$), we can express the M-replicated partition function as

$$\mathscr{Z}^{(M)} = \int \hat{\mathscr{D}}\tilde{\varphi}_i\, \hat{\mathscr{D}}\varphi_i \left\langle \exp\left\{ \sum_{j=1}^{M} \left[\int d^dx\, dt \sum_{\alpha=1}^{2} (\tilde{h}_{j\alpha}\tilde{\varphi}_{j\alpha} + h_{j\alpha}\varphi_{j\alpha}) - \hat{\mathscr{H}} \right] \right\} \right\rangle_{\mathrm{RA}}$$

$$= \int \hat{\mathscr{D}}\tilde{\varphi}_i\, \hat{\mathscr{D}}\varphi_i \exp\left[\sum_{j=1}^{M} \int d^dx\, dt \sum_{\alpha=1}^{2} (\tilde{h}_{j\alpha}\tilde{\varphi}_{j\alpha} + h_{j\alpha}\varphi_{j\alpha}) - \hat{\mathscr{H}}^{(M)} \right]$$

$$\hat{\mathscr{H}}^{(M)} \equiv \sum_{j=1}^{M} \int d^dx\, dt \sum_{\alpha=1}^{2} \Big[\lambda_b^{-1}\tilde{\varphi}_{j\alpha}^2 + i\tilde{\varphi}_{j\alpha}(\lambda_b^{-1}\partial/\partial t - \nabla_\perp^2 - a_b^2\nabla_\parallel^2 + r_b)\varphi_{j\alpha}$$

$$+ (i/3!)\hat{u}_s\tilde{\varphi}_{j\alpha}\varphi_{j\alpha} \sum_{k=1}^{M}\sum_{\beta=1}^{2} \varphi_{k\beta}^2 + (i/3!)\hat{u}_c\tilde{\varphi}_{j\alpha}\varphi_{j\alpha}^3 \Big]$$

$$+ 2\Delta \sum_{j,k=1}^{M}\sum_{\alpha,\beta=1}^{2} \int d^dx\, d^dy\, dt\, dt'\, \delta^d(x-y)\, \tilde{\varphi}_{j\alpha}(x,t)$$

$$\times \varphi_{j\alpha}(x,t)\, \tilde{\varphi}_{k\beta}(y,t')\, \varphi_{k\beta}(y,t') \tag{2.9}$$

where $\hat{\mathscr{D}}\varphi_i \equiv \prod_{i=1}^{M} \mathscr{D}\varphi_i = \prod_{i=1}^{M}\prod_{\alpha=1}^{2} d\varphi_{i\alpha}$. Therefore, from the effective generating functional averaged over the random potentials

$$F(\tilde{h}, h) \equiv \langle \mathscr{F}(\tilde{h}, h)\rangle_{\mathrm{RA}} = -\lim_{M\to 0} M^{-1} \ln \mathscr{Z}^{(M)}(\tilde{h}, h) \tag{2.10}$$

we can generate the cumulant Green's function $G^{(\tilde{n},n)}$

$$F(\tilde{h}, h) = \sum_{\tilde{n},n} (\tilde{n}!n!)^{-1} \int \mathscr{D}(\tilde{x}\tilde{t})\, \mathscr{D}(xt)\, G^{(\tilde{n},n)}_{\{\tilde{x}\}\{\alpha\}}(\tilde{x}_{\tilde{1}}\tilde{t}_{\tilde{1}}, \ldots, x_n t_n)$$

$$\times \tilde{h}_{\tilde{\alpha}_{\tilde{1}}}(\tilde{x}_{\tilde{1}}\tilde{t}_{\tilde{1}}) \cdots \tilde{h}_{\tilde{\alpha}_{\tilde{n}}}(\tilde{x}_{\tilde{n}}\tilde{t}_{\tilde{n}})\, h_{\alpha_1}(x_1 t_1) \cdots h_{\alpha_n}(x_n t_n) \tag{2.11}$$

To reduce the number of diagrams to calculate, using the Legendre transformation

$$\Gamma(\tilde{\varphi}, \varphi) \equiv F(\tilde{h}, h) + \int d^dx\, dt \sum_{\alpha=1}^{2} [\tilde{h}_\alpha\tilde{\varphi}_\alpha + h_\alpha\varphi_\alpha] \tag{2.12}$$

we can derive the one-particle irreducible vertex functions $\Gamma^{(\tilde{n},n)}$ and the equations of motion

$$\Gamma(\tilde{\varphi}, \varphi) \equiv \sum_{\tilde{n},n} (\tilde{n}!n!)^{-1}\, \Gamma^{(\tilde{n},n)}\tilde{\varphi}^{\tilde{n}}\varphi^n$$

$$\tilde{h}_\alpha(x,t) = \delta\Gamma/\delta\tilde{\varphi}_\alpha(x,t), \qquad h_\alpha(x,t) = \delta\Gamma/\delta\varphi_\alpha(x,t) \tag{2.13}$$

The static vertex functions and free energy are evaluated as the limit of zero external frequencies

$$\Gamma^{(n)}(q_1,\ldots,q_n)=\Gamma^{(1,n-1)}(q_1,\ldots,q_n,\{\omega=0\})$$

$$F(M)-F(0)=\sum_{n=1}^{\infty}(n!)^{-1}M^n\Gamma^{(1,n-1)}(\{q=0\},\{\omega=0\}) \tag{2.14}$$

Finally the tensorial structures of interactions in the effective Hamiltonian (2.9) and the diagrammatic rules in the perturbation expansion were summarized (Fig. 1). In Fig. 1 the interactions $\{u_s, u_c, \text{ and } \Delta\}$ (designated $\{u\}$)

$$\hat{u}_s(i,j,k,l)\equiv\hat{u}_s S_{ijkl}, \qquad S_{ijkl}\equiv\frac{1}{3}(\delta_{ij}\delta_{kl}+\delta_{ik}\delta_{jl}+\delta_{il}\delta_{jk})$$

$$\hat{u}_c(i,j,k,l)\equiv\hat{u}_c C_{ijkl}, \qquad C_{ijkl}\equiv\delta_{ij}\delta_{kl}\delta_{ik}$$

$$\Delta(ij;kl)\equiv\Delta D_{ijkl}, \qquad D_{ijkl}\equiv\delta_{ij}\delta_{kl} \tag{2.15}$$

are drawn by ●, □, and ..., respectively, and are associated with the vertices $\Gamma_{g_s}^{(1,3)}$, $\Gamma_{g_c}^{(1,3)}$, and $\Gamma_{\delta}^{(2,2)}$, respectively. In diagrammatic expansion all

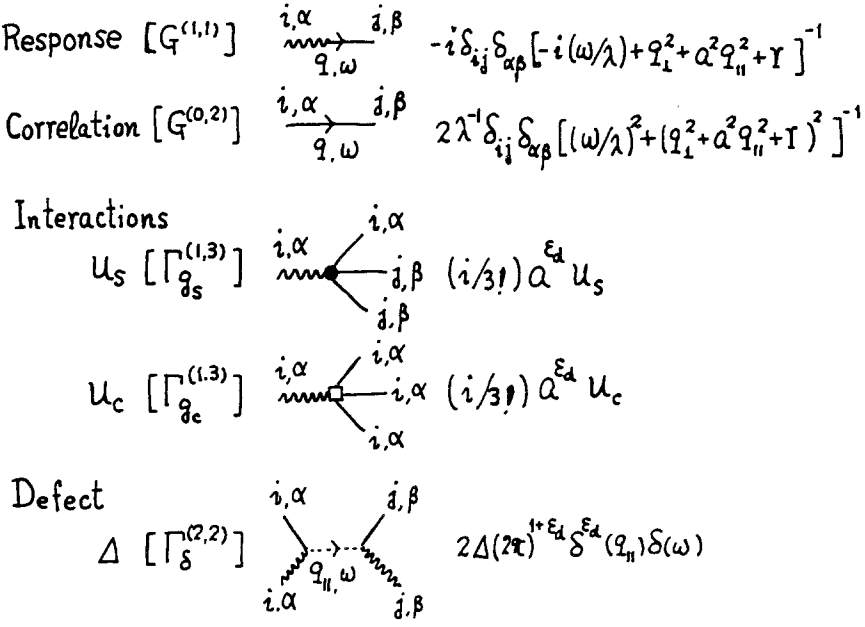

Fig. 1. Diagram elements constructed by the Hamiltonian (2.9).

diagrams conserve momentum and frequency at each vertex of u_s and u_c, while the defect vertex Δ requires the constraint $(2\pi)^{1+\varepsilon_d}\delta^{\varepsilon_d}(q_\parallel)\,\delta(\omega)$. In dynamics causality plays an important role necessitating all closed-loop diagrams constructed with two or more response lines to vanish. Furthermore, we can omit the tadpole diagrams including a single response line, which are rigorously canceled by the Jacobian term.

3. RENORMALIZATION AND ITS CONSTANTS

Using the effective Hamiltonian (2.9), together with the generating functional (2.13), we expanded the Feynman diagrams for the correlation and response vertices $\{\Gamma^{(1,1)}, \Gamma^{(1,3)}_{g_s}, \Gamma^{(1,3)}_{g_c}, \Gamma^{(2,2)}_{\delta}$, and so on$\}$ (designated $\{\Gamma^{(\tilde{n},n)}\}$), in order to study critical behavior of the systems. As the Feynman diagrams have singularities as $\{\varepsilon\} \to 0$ [$\{\varepsilon\}$ stands for the set of ε and $\tilde{\varepsilon}$ $(\equiv \varepsilon + \varepsilon_d)$] in the integrals over the momenta despite a relevant beneath four dimensions according to dimensional analysis, we used the dimensional regularization of 't Hooft *et al.*[19] and determined the renormalized fields, interactions, and vertices.

Initially, the renormalization constants $\{Z_\varphi, Z_{a^2}, Z_t, Z_\lambda, Z_{g_s}, Z_{g_c}, Z_\delta\}$ (designated $\{Z\}$) are defined

$$\varphi_b = Z_\varphi^{1/2}\varphi_R, \qquad \tilde{\varphi}_b = Z_\varphi^{1/2}\tilde{\varphi}_R, \qquad a_b^2 = Z_{a^2}a_R^2$$
$$r_b = r_{bc} + \kappa^2 Z_t t, \qquad \lambda_b^{-1} = \kappa^2 Z_\lambda \lambda^{-1}$$
$$u_{sb} = \kappa^\varepsilon K_d^{-1} Z_{g_s} g_s, \qquad u_{cb} = \kappa^\varepsilon K_d^{-1} Z_{g_c} g_c, \qquad \Delta_b = \kappa^{\tilde{\varepsilon}} K_{\tilde{d}}^{-1} Z_\delta \delta \tag{3.1}$$

then the renormalized vertices are related to the bare vertices as

$$\Gamma^{(\tilde{n},n)}(\{p\}, \{\omega\}, g_s, g_c, \delta, a_R^2, t, \lambda, \kappa)$$
$$= Z_\varphi^{(\tilde{n}+n)/2}\Gamma_b^{(\tilde{n},n)}(\{p\}, \{\omega\}, u_{sb}, u_{cb}, \Delta_b, a_b^2, r_b, \lambda_b) \tag{3.2}$$

where the subscripts R and b stand for the renormalized and bare quantities, respectively, and $K_d \equiv 2\pi^{d/2}/(2\pi)^d\,\Gamma(d/2)$. To make the renormalized interactions $\{g_s, g_c, \delta\}$ (designated $\{g\}$) dimensionless, a renormalization parameter κ with momentum unit was introduced. As all renormalization constants $\{Z\}$ and bare vertices $\{\Gamma^{(\tilde{n},n)}\}$ are Feynman expanded as power series in $\{g\}$, the renormalized vertices are also expressed by the polynomial form of the renormalized interactions $\{g\}$. That is, (1) the Feynman diagrams for the vertices $\{\Gamma^{(\tilde{n},n)}\}$ with respect to the bare interactions $\{u\}$ were expanded; (2) the bare interactions ($\{a_b^2, \lambda_b^{-1}\}$ and $\{u\}$) were replaced by renormalized ones times the renormalization constant according to (3.1); and (3) the Feynman integrals were evaluated.

Seven renormalization constants $\{Z\}$ were determined so that the associated renormalized-vertex functions became finite, i.e., the coefficients of $\{Z\}$ canceled the poles in $\{\varepsilon\}$ at each order of $\{g\}$. Each coefficient of the renormalization constants $\{Z_\varphi, Z_{a^2}, Z_t, Z_\lambda\}$ is explicitly determined by the elimination of the poles in $\{\varepsilon\}$ arising in the vertices $\{\partial\Gamma^{(1,1)}/\partial p_\perp^2, \partial\Gamma^{(1,1)}/\partial p_\parallel^2, \Gamma^{(1,1)}, \partial\Gamma^{(1,1)}/\partial\omega\}$. Here $\Gamma^{(1,1)}$ means identity expressed by both sides of (3.2) with $\tilde{n}=1=n$, and the values of four cases are evaluated at zero external frequency ω and zero momentum p. Similarly, the renormalization constants $\{Z_{g_s}, Z_{g_c}, Z_\delta\}$ are determined, so as to remove the poles appearing in the vertices $\{\Gamma_{g_s}^{(1,3)}, \Gamma_{g_c}^{(1,3)}, \Gamma_\delta^{(2,2)}\}$ [expressed by (3.3)], at the four zero external frequencies and zero momenta. It is remarkable that (i) three vertices $\{\Gamma_{g_s}^{(1,3)}, \Gamma_{g_c}^{(1,3)}, \Gamma_\delta^{(2,2)}\}$ have similar characteristics to those of the interactions $\{g\}$ with respect to the tensorial structure of spin and replica indices and to the δ functions of the external frequencies and momenta; (ii) all renormalization constants $\{Z\}$ are determined order by order in ε and $\tilde{\varepsilon}$; and (iii) the renormalization constants (except Z_λ) are the same as those obtained in the static case.

The explicit diagrams and their contributions for the vertices $\{\Gamma^{(\tilde{n},n)}\}$ are listed in Appendix A (Figs. A1, A2 and Tables AI, AII). Using the dimensional regularization in these expressions, the renormalization constants $\{Z\}$ were obtained:

$$Z_\varphi = 1 - \frac{1}{36\varepsilon} g_s^2 - \frac{1}{12\varepsilon} g_s g_c - \frac{1}{48\varepsilon} g_c^2 + \frac{4}{3(\varepsilon+\tilde{\varepsilon})} g_s\delta + \frac{1}{\varepsilon+\tilde{\varepsilon}} g_c\delta - \frac{2}{\tilde{\varepsilon}}\delta^2$$

$$Z_{a^2} = 1 - \frac{2}{\tilde{\varepsilon}}\delta$$

$$Z_t = 1 + \frac{2}{3\varepsilon} g_s + \frac{1}{2\varepsilon} g_c - \frac{4}{\tilde{\varepsilon}}\delta$$

$$Z_\lambda = 1 - \frac{4}{\tilde{\varepsilon}}\delta$$

$$\begin{aligned} Z_{g_s} = 1 &+ \frac{5}{3\varepsilon} g_s + \frac{1}{\varepsilon} g_c - \frac{24}{\tilde{\varepsilon}}\delta + \left(\frac{25}{9\varepsilon^2} - \frac{5}{6\varepsilon}\right) g_s^2 + \left(\frac{21-\varepsilon 5}{6\varepsilon^2}\right) g_s g_c \\ &+ \left[\frac{5(6-\varepsilon)}{24\varepsilon^2}\right] g_c^2 + \frac{1}{3\varepsilon\tilde{\varepsilon}(\varepsilon+\tilde{\varepsilon})}\left[-216\varepsilon - 240\tilde{\varepsilon} - 18\varepsilon^2 + 178\varepsilon\tilde{\varepsilon}\right] g_s\delta \\ &+ \frac{2}{\varepsilon\tilde{\varepsilon}(\varepsilon+\tilde{\varepsilon})}\left(-24\varepsilon - 20\tilde{\varepsilon} - 2\tilde{\varepsilon}^2 + 19\varepsilon\tilde{\varepsilon} - 2\tilde{\varepsilon}^2\right) g_c\delta \\ &+ \frac{4}{\tilde{\varepsilon}^2}\left[120 + 4\varepsilon - 45\tilde{\varepsilon}\right]\delta^2 \end{aligned}$$

$$Z_{g_c} = 1 + \frac{2}{\varepsilon} g_s + \frac{3}{2\varepsilon} g_c - \frac{24}{\tilde{\varepsilon}} \delta + \left(\frac{11}{3\varepsilon^2} - \frac{23}{18\varepsilon} \right) g_s^2 + \left[\frac{11(3-\varepsilon)}{6\varepsilon^2} \right] g_s g_c$$
$$+ \left(\frac{54 - 17\varepsilon}{24\varepsilon^2} \right) g_c^2 + \frac{2}{3\varepsilon\tilde{\varepsilon}(\varepsilon + \tilde{\varepsilon})} (-120\varepsilon - 144\tilde{\varepsilon} - 10\varepsilon^2 + 102\varepsilon\tilde{\varepsilon})\, g_s \delta$$
$$+ \frac{1}{\varepsilon\tilde{\varepsilon}(\varepsilon + \tilde{\varepsilon})} [-12(5\varepsilon + 6\tilde{\varepsilon}) - (5\varepsilon - 51\tilde{\varepsilon})\varepsilon]\, g_c \delta + \frac{4}{\tilde{\varepsilon}^2} [120 + 4\varepsilon - 45\tilde{\varepsilon}] \delta^2$$
$$Z_\delta = 1 + \frac{4}{3\varepsilon} g_s + \frac{1}{\varepsilon} g_c - \frac{16}{\tilde{\varepsilon}} \delta + \frac{36 - 5\varepsilon}{18\varepsilon^2} g_s^2 + \frac{10 - 2\varepsilon}{3\varepsilon^2} g_s g_c + \frac{5(6-\varepsilon)}{24\varepsilon^2} g_c^2$$
$$+ \frac{-\varepsilon^2 + 6\varepsilon\tilde{\varepsilon} - 6\varepsilon - 14\tilde{\varepsilon}}{\varepsilon\tilde{\varepsilon}(\varepsilon + \tilde{\varepsilon})} \left(\frac{4}{3} g_s + g_c \right) \delta + \frac{10(4 - \tilde{\varepsilon})}{\tilde{\varepsilon}^2} \delta^2 \tag{3.3}$$

4. RG EQUATIONS AND CRITICAL BEHAVIOR

Of interest here are the static critical behavior in the equilibrium and the dynamic critical behavior in the relaxation process. Such critical behaviors are measured in the $\perp$ and $\parallel$ directions experimentally through correlation, susceptibility, and specific heat measurements, neutron scattering, and so on. These physical quantities were then theoretically investigated in the vertex functions $\Gamma^{(1,n-1)}$ as a function of the correlation length. The behavior is evaluated by the RG equations

$$[\mathscr{D} - \tfrac{1}{2} n \eta\{g\}] \Gamma^{(1,n-1)}(\{p\}, \{\omega\}, \{g\}, a^2, t, \lambda, \kappa) = 0 \quad \text{for } n(\geqslant 1) \text{ integer} \tag{4.1}$$

where

$$\mathscr{D} \equiv \kappa(\partial/\partial\kappa)|_{\text{bare}} = \kappa\partial/\partial\kappa + \beta\{g\}\partial/\partial g - \gamma_{a^2}\{g\} a^2 \partial/\partial a^2$$
$$- \gamma_t\{g\} t\partial/\partial t + \zeta\{g\}\lambda\partial/\partial\lambda$$
$$\beta\{g\}\partial/\partial g \equiv \beta_s\{g\}\partial/\partial g_s + \beta_c\{g\}\partial/\partial g_c + \beta_\delta\{g\}\partial/\partial\delta$$
$$\eta\{g\} \equiv \mathscr{D} \ln Z_\varphi\{g\}, \qquad \gamma_{a^2}\{g\} \equiv \mathscr{D} \ln Z_{a^2}\{g\}, \qquad \gamma_t\{g\} \equiv \mathscr{D} \ln Z_t\{g\}$$
$$\zeta\{g\} \equiv \mathscr{D} \ln Z_\lambda\{g\} \tag{4.2}$$

By substituting the expressions (3.3) into (4.2), we obtained the expressions for $\{\beta_s, \beta_c, \beta_\delta\}$ (designated $\{\beta\}$) and $\{\eta, \gamma_{a^2}, \gamma_t, \zeta\}$

$$-\beta_s/g_s = \varepsilon - \frac{5}{3}g_s - g_c + 24\delta + \frac{5}{3}g_s^2 + \frac{5}{3}g_s g_c + \frac{5}{12}g_c^2$$
$$+ 2\left(3\frac{\varepsilon}{\tilde{\varepsilon}} - \frac{89}{3}\right)g_s\delta + 2\left(4\frac{\tilde{\varepsilon}}{\varepsilon} - 19\right)g_c\delta + 8\left(45 - 4\frac{\varepsilon}{\tilde{\varepsilon}}\right)\delta^2$$

$$-\beta_c/g_c = \varepsilon - 2g_s - \frac{3}{2}g_c + 24\delta + \frac{23}{9}g_s^2 + \frac{11}{3}g_s g_c + \frac{17}{12}g_c^2$$
$$+ \left(5\frac{\varepsilon}{\tilde{\varepsilon}} - 51\right)\left[\frac{4}{3}g_s + g_c\right]\delta + 8\left(45 - 4\frac{\varepsilon}{\tilde{\varepsilon}}\right)\delta^2$$

$$-\beta_\delta/\delta = \tilde{\varepsilon} - \frac{4}{3}g_s - g_c + 16\delta + \frac{5}{9}g_s^2 + \frac{4}{3}g_s g_c + \frac{5}{12}g_c^2$$
$$+ 2\left(2\frac{\varepsilon}{\tilde{\varepsilon}} - 13\right)\left(\frac{4}{3}g_s + g_c\right)\delta + 168\delta^2 \tag{4.3}$$

$$\eta = \tfrac{1}{18}g_s^2 + \tfrac{1}{6}g_s g_c + \tfrac{1}{24}g_c^2 - \tfrac{4}{3}g_s\delta - g_c\delta + 4\delta^2$$
$$\gamma_{a^2} = 2\delta$$
$$\gamma_t = 2 - \tfrac{2}{3}g_s - \tfrac{1}{2}g_c + 4\delta$$
$$\zeta = 2 + 4\delta \tag{4.4}$$

At the critical point, since the correlation length ξ is infinite, the physical properties should be invariant for any change of the scale parameter κ ($\kappa^{-1} < \xi$). That condition is satisfied when

$$\beta_s\{g^*\} = \beta_c\{g^*\} = \beta_\delta\{g^*\} = 0 \tag{4.5}$$

The interactions $\{g^*\}$ are designated the fixed point. It consists of the Gaussian system G, regular XY (Ising) system P_{XY} (P_I), unphysical system U, extended defect XY (Ising) system D_{XY} (D_I), and extended defect (regular) system with cubic anisotropy D^c_{XY} (P^c_{XY}). Their expressions of single loop order, for simplicity, were obtained as follows:

		g_s^*	g_c^*	δ^*	
(i)	G	0	0	0	
(ii)	P_{XY}	$\frac{3}{5}\varepsilon$	0	0	
(iii)	P_I	0	$\frac{2}{3}\varepsilon$	0	
(iv)	U	0	0	$-\frac{1}{16}\tilde{\varepsilon}$	
(v)	P^c_{XY}	ε	$-\frac{2}{3}\varepsilon$	0	
(vi)	D_{XY}	$\frac{3}{2}(3\tilde{\varepsilon} - 2\varepsilon)$	0	$\frac{1}{16}(5\tilde{\varepsilon} - 4\varepsilon)$	
(vii)	D_I	0	$16\delta_I^*$	δ_I^*	(4.6.1)
(viii)	D^c_{XY}	$24\delta^*_{XY}$	$-16\delta^*_{XY}$	δ^*_{XY}	(4.6.2)

where $\delta_I^* \equiv 1/2 \cdot [3\tilde{\varepsilon}(3\tilde{\varepsilon}-2\varepsilon)/2(89\tilde{\varepsilon}-36\varepsilon)]^{1/2}$ and $\delta_{XY}^* \equiv [3\tilde{\varepsilon}(3\tilde{\varepsilon}-2\varepsilon)/8(353\tilde{\varepsilon}-36\varepsilon)]^{1/2}$ with a selected solution of $\delta^* > 0$. The fixed points (i)–(v) have already been studied. In the two remaining cases, as the determinant $\{-\beta/g\}$ expressed by (4.3) is degenerate in order $\{\varepsilon\}$ but nondegenerate in order $\{\varepsilon^2\}$, the effective interactions $\{g^*\}$ were obtained in the $\{\varepsilon^{1/2}\}$-expansion form. The fixed points (vi)–(vii), which were studied by Dorogovtsev,[10] Boyanovsky *et al.*,[11] and Lawrie *et al.*,[12] coincide with those for $\varepsilon_d = 0$. The final fixed point (viii) gives new results.

The results further indicate that (1) P_{XY}, P_I, and D_{XY} always have positive interactions for the physical dimensions (ε and $\tilde{\varepsilon}$ positive); (2) U never occurs because its interaction is always negative; (3) The g_c interaction of P_{XY}^c and D_{XY}^c is negative, i.e., their systems choose the easy axes along $(\pm 1, 0)$ or $(0, \pm 1)$ directions; and (4) D_I and D_{XY}^c have positive real values δ^* for $\tilde{\varepsilon} > \frac{2}{3}\varepsilon$.

System stability near the critical point can be investigated by the eigenvalues of the matrix of the derivatives of $\beta_i \in \{\beta\}$ with respect to $g_j \in \{g\}$, $\partial\beta_i/\partial g_j$, at the fixed points:

$$
\begin{aligned}
&\text{(i)} \quad G\colon \lambda_s = -\varepsilon, \qquad \lambda_c = -\varepsilon, \qquad \lambda_\delta = -\tilde{\varepsilon} \\
&\text{(ii)} \quad P_{XY}\colon \lambda_s = \varepsilon, \qquad \lambda_c = \varepsilon/5, \qquad \lambda_\delta = -(5\tilde{\varepsilon}-4\varepsilon)/5 \\
&\text{(iii)} \quad P_I\colon \lambda_s = -\varepsilon/3, \qquad \lambda_c = \varepsilon, \qquad \lambda_\delta = -(3\tilde{\varepsilon}-2\varepsilon)/3 \\
&\text{(iv)} \quad U\colon \lambda_s = (3\tilde{\varepsilon}-2\varepsilon)/2 = \lambda_c, \qquad \lambda_\delta = \tilde{\varepsilon} \\
&\text{(v)} \quad P_{XY}^c\colon \lambda_1 = \varepsilon, \qquad \lambda_2 = -\varepsilon/3, \qquad \lambda_\delta = -(3\tilde{\varepsilon}-2\varepsilon)/3 \\
&\text{(vi)} \quad D_{XY}\colon \lambda_1, \qquad \lambda_2 = \tfrac{1}{8}[A \pm (A^2-B)^{1/2}], \qquad \lambda_c = (3\tilde{\varepsilon}-2\varepsilon)/2 \\
&\qquad\qquad \text{with } A \equiv 2[(3\varepsilon+\varepsilon_d)+4\varepsilon_d], \quad B \equiv 32(\varepsilon+3\varepsilon_d)(\varepsilon+5\varepsilon_d) \\
&\text{(vii)} \quad D_I\colon \lambda_s = -8\delta_I^*, \qquad \lambda_1 = 0, \qquad \lambda_2 = 8\delta_I^* \\
&\text{(viii)} \quad D_{XY}^c\colon \lambda_1 = -8\delta_{XY}^*, \qquad \lambda_2 = 0, \qquad \lambda_3 = 8\delta_{XY}^*
\end{aligned}
\tag{4.7}
$$

Here λ_s, λ_c, and λ_δ stand for the eigenvalues in the direction of the axes g_s, g_c, and δ, respectively, and λ_1, λ_2, and λ_3 denote the eigenvalues in the direction of the orthogonal axes (eigenvectors). The values of δ^* in the $\varepsilon^{1/2}$-expanded systems have been expressed in the corresponding fixed points. A stable fixed point against the long-range fluctuations has positive eigenvalues, and is characterized by an ingoing flow for increasing correlation length. The fixed point G (U) is unstable (stable) for any interaction of $\{g\}$ and the tendency in the δ-direction strengths with increasing ε_d. The fixed point P_{XY} (P_I) is stable for the interactions of g_s and g_c (g_c), while the instability of both systems becomes significant for the δ interaction with

increasing ε_d. The fixed point P^c_{XY} is stable only along one direction of eigenvectors on the g_s–g_c plane, while instability along the other eigenvectors heightens with increasing ε and ε_d. The fixed point D_{XY} has interesting features: It is the most stable, having three positive real eigenvalues for the dimensions $0 \leqslant \varepsilon_d \leqslant \varepsilon/[17+(384)^{1/2}]$ (i.e., $0 \leqslant \varepsilon_d/\varepsilon < 0.02733$) but two complex eigenvalues with positive real part in addition to one positive real eigenvalue for the dimensions $\varepsilon_d/\varepsilon > 1/[17+(384)^{1/2}]$. This reveals the fact that flows in the interaction space approach the fixed point monotonously in the former case but spirally in the latter case. Fixed point D_I is unstable for the g_s interaction; it is marginal in one direction and stable in the other direction, of the orthogonal axes on the $g_c - \delta$ plane. Fixed point D^c_{XY} has stable, marginal, and unstable eigenvalues in certain directions of three orthogonal axes. Note that in the regular systems the system P_{XY} is the most stable, but with the appearance of defects the extended defect system D_{XY} becomes the most stable. Its flow trajectories approach the fixed point D_{XY} nonoscillatory for small $\varepsilon_d/\varepsilon$ but spirally for large $\varepsilon_d/\varepsilon$.

The fixed points and the flow trajectories are summarized in Appendix B and drawn schematically in Fig. 2.

The critical behavior of the physical quantities of the systems can be evaluated by the scale transformation of all external momenta ($p_\perp \to \kappa p_\perp$, $p_\parallel \to a^{-1}\kappa p_\parallel$) and frequencies ($\omega \to \lambda\omega$) in the vertices $\Gamma^{(1,n-1)}$. By recalling the definition of $\Gamma^{(1,n-1)}$ ($\equiv$ set of the one-particle irreducible diagrams of $G^{(1,n-1)}/\prod^n[G^{(1,1)}]$) and the dimensional relations (2.3a), we get the dimensional expression

$$\begin{aligned}[\Gamma^{(1,n-1)}] &= [\kappa^{((d-2)/2)n}\,\kappa^{-d(n-1)}][\kappa^{((d-2)/2)2}\,\kappa^{-d}]^{-n}[a^{-(\varepsilon_d/2)n+\varepsilon_d(n-1)}] \\ &\quad \times [a^{-(\varepsilon_d/2)2+\varepsilon_d}]^{-n}[\lambda^0][\lambda^0]^{-n} \\ &= [\kappa^{d_n} a^{e_n} \lambda^0] \end{aligned} \tag{4.8}$$

where $d_n \equiv d - n(d-2)/2$ and $e_n \equiv (n-2)\varepsilon_d/2$. Thus the renormalized vertex functions $\Gamma^{(1,n-1)}$ have the same dependence as $\Gamma^{(n)}$, with respect to the parameters:

$$\begin{aligned}&\Gamma^{(1,n-1)}(\{\kappa p_\perp, a^{-1}\kappa p_\parallel\}, \{\lambda\omega\}, \{g\}, a^2, t, \lambda, \kappa) \\ &\quad = \kappa^{d_n} a^{e_n} \Gamma^{(n)}(\{p_\perp, p_\parallel\}, \{\omega\}, \{g\}, t)\end{aligned} \tag{4.9}$$

On the other hand, the renormalization constants are independent of a^2, t, λ, and κ. The behavior of the vertices $\Gamma^{(1,n-1)}$ can be described with the RG equations

$$\begin{aligned}&[\zeta\tilde{l}\partial/\partial\tilde{l} + l\partial/\partial l + \xi a^2 \partial/\partial a^2 - \beta\{g\}\partial/\partial g + \gamma_t t\partial/\partial t + n(d-\varepsilon_d+\xi\varepsilon_d-2+\eta)/2 \\ &\quad -(d-\varepsilon_d+\xi\varepsilon_d)]\,\Gamma^{(n)}(\{lp_\perp, ap_\parallel\}, \{\tilde{l}\omega\}, \{g\}, t) = 0\end{aligned} \tag{4.10}$$

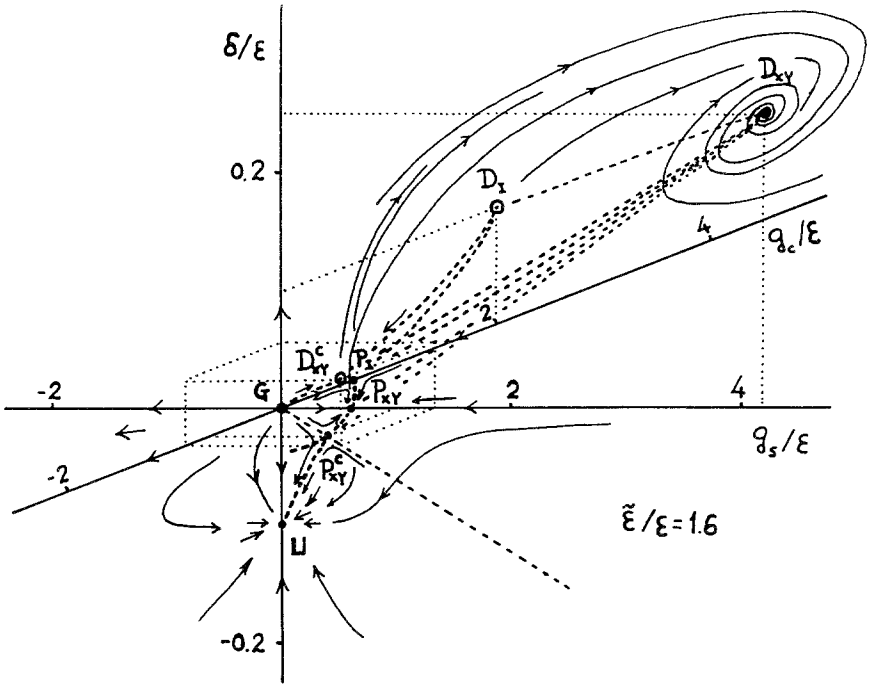

Fig. 2. Fixed points and schematic trajectories of flows in the interaction space (g_s, g_c, δ). The ε-expanded fixed points (i.e., the Gaussian $[G]$, regular XY $[P_{XY}]$, regular Ising $[P_I]$, unphysical $[U]$, regular XY with cubic anisotropy $[P^c_{XY}]$ and extended defect XY $[D_{XY}]$) are denoted by ●, and the $\varepsilon^{1/2}$-expanded ones (i.e., the extended defect Ising $[D_I]$ and extended defect XY with cubic anisotropy $[D^c_{XY}]$) are marked by ⊙. In the regular systems (without defects $\delta = 0$) the XY system P_{XY} is most stable; with the appearance of defects the extended defect XY system D_{XY} becomes most stable.

where $\{\tilde{I}, I\}$ are arbitrary dimensionless parameters and

$$\xi\{g\} = 1 + \gamma_{a^2}\{g\} \tag{4.11}$$

The solution of the RG equations at the fixed point describes system behavior at (near) the critical temperature $t = 0$ $(t \gtrless 0)$:

$$\Gamma^{(n)}(\{p_\perp, ap_\parallel\}, \{\omega\}, \{g^*\}, t) = t^{2-\alpha-n\beta}\, g^{(n)}(\{t^{-\nu_\perp} p_\perp, t^{-\nu_\parallel} ap_\parallel\}, \{t^{-\lambda}\omega\})$$

with

$$\nu_\perp \equiv \gamma_t^{-1}\{g^*\},\ \nu_\parallel \equiv \xi\nu_\perp, \qquad \gamma \equiv (2-\eta)\nu_\perp$$
$$2-\alpha \equiv (d-\varepsilon_d)\nu_\perp + \varepsilon_d\nu_\parallel, \qquad 2\beta \equiv 2-\alpha-\gamma, \qquad \lambda \equiv \zeta\nu_\perp \tag{4.12}$$

where $\xi \equiv \xi\{g^*\}$, $\eta \equiv \eta\{g^*\}$, $\zeta \equiv \zeta\{g^*\}$, and $g^{(n)}$ stand for the homogeneous functions. Similarly, the free energy of the systems ($n=0$) is expressed for $t<0$ as

$$F(M, t) = t^{2-\alpha} f(Mt^{-\beta}) \qquad (t \equiv |-t|) \tag{4.13}$$

and the response function, $G^{(2)} \equiv 1/\Gamma^{(2)}$, behaves as

$$G^{(2)}(p_\perp, p_\parallel, \omega, t) = t^{-\gamma} \hat{g}_2(t^{-\nu_\perp} p_\perp\, t^{-\nu_\parallel} a p_\parallel, t^{-\lambda}\omega) \tag{4.14.1}$$

near the critical point, and just at the critical temperature ($t=0$)

$$G^{(2)}(p_\perp, p_\parallel, \omega, 0) = \begin{cases} |p_\perp|^{\eta_\perp - 2} g_{2\perp}(a p_\parallel |p_\perp|^{-\xi}, \omega |p_\perp|^{-z_\perp}) \\ |a p_\parallel|^{\eta_\parallel - 2} g_{2\parallel}(p_\perp |a p_\parallel|^{-1/\xi}, \omega |a p_\parallel|^{-z_\parallel}) \end{cases} \tag{4.14.2}$$

where

$$2 - \eta_\perp = \xi(2 - \eta_\parallel) = 2 - \eta, \qquad z_\perp = \xi z_\parallel = \lambda/\nu_\perp = \zeta \tag{4.15}$$

and $\{f, \hat{g}_2, g_{2\perp}, g_{2\parallel}\}$ denote the homogeneous functions. The critical exponents $\{\eta_\perp, \nu_\perp, z_\perp\}$ and $\{\eta_\parallel, \nu_\parallel, z_\parallel\}$ are associated with those in the medium perpendicular and parallel to the extended defects.

The explicit expressions of single-loop order for the critical exponents are given by

$$\begin{gathered} \eta_\perp = 0, \qquad \eta_\parallel = 4\delta^*, \qquad \nu_\perp = \tfrac{1}{2}(1 + 2\delta^*), \qquad \nu_\parallel = \tfrac{1}{2}(1 + 4\delta^*) \\ \gamma = 1 + 2\delta^*, \qquad 2 - \alpha = 2(1 + 2\delta^*), \qquad 2\beta = 1 + 2\delta^* \\ z_\perp = 2(1 + 2\delta^*), \qquad z_\parallel = 2, \qquad \lambda = 1 + 4\delta^* \end{gathered} \tag{4.16}$$

using

$$\begin{gathered} \eta = -33\delta^2 = 0 + O(\{\varepsilon\}), \qquad \gamma_{a^2} = 2\delta^*, \qquad \gamma_t = 2(1 - 2\delta^*) \\ \zeta = 2(1 + 2\delta^*), \qquad \xi = 1 + 2\delta^* \end{gathered} \tag{4.17}$$

where the values of η are negative in two-loop order but null in single-loop order.

The values of these critical exponents of the extended (pointlike) defect-XY systems with $\varepsilon_d > 0$ ($\varepsilon_d = 0$) are tabulated in Table I(a) and I(b) for $\varepsilon = 1$ and $\varepsilon = 2$, respectively. For comparison, those of the regular isotropic (cubic anisotropic) systems are tabulated in Table I(c) (I(d)), which have been obtained by LeGuillou *et al.*[20] (Yamazaki[18]) up to the order of ε^2. Here it should be recalled that (1) in the pointlike defect systems a parallel component of the critical exponents does not exist; (2) in

Table I. Comparison of Critical Exponent Values of the Extended Defect *XY* Systems with Those of the Pointlike Defect-*XY* Systems and the Regular (Isotropic and Cubic Anisotropic)-*XY* Systems[a]

ε_d	δ^*	φ	$\nu_\perp$	$\nu_\parallel$	γ	$\eta_\perp$	$\eta_\parallel$	ξ	$z_\perp$	$z_\parallel$	α
					Case (a): $\varepsilon = 1$, $N = 2$						
0	0.034	0.244	0.534		1.069	0			2.138		−0.138
0.2	0.043	0.360	0.543	0.586	1.086	0	0.172	1.086	2.172	2	−0.172
0.4	0.050	0.477	0.550	0.600	1.100	0	0.201	↑	2.201	2	−0.201
0.6	0.056	0.594	0.556	0.613	1.113	0	0.226		2.226	2	−0.226
0.8	0.062	0.710	0.562	0.624	1.124	0	0.248		2.248	2	−0.248
1.0	0.067	0.827	0.567	0.634	1.134	0	0.268	γ	2.268	2	−0.268
1.2	0.072	0.944	0.572	0.643	1.143	0	0.286		2.286	2	−0.286
1.4	0.076	1.060	0.576	0.652	1.152	0	0.304		2.304	2	−0.304
1.6	0.080	1.177	0.580	0.660	1.160	0	0.320		2.320	2	−0.320
1.8	0.084	1.294	0.584	0.668	1.168	0	0.336	↓	2.336	2	−0.336
2.0	0.088	1.352	0.588	0.676	1.176	0	0.351	1.176	2.351	2	−0.351
					Case (b): $\varepsilon = 2$, $N = 2$						
0	0.046	0.309	0.549		1.097	0			2.195		−0.195
0.2	0.055	0.442	0.555	0.610	1.110	0	0.221	1.110	2.221	2	−0.221
0.4	0.061	0.575	0.561	0.622	1.122	0	0.244	↑	2.244	2	−0.244
0.6	0.066	0.709	0.566	0.632	1.132	0	0.265		2.265	2	−0.265
0.8	0.071	0.842	0.571	0.642	1.142	0	0.284		2.284	2	−0.284
1.0	0.076	0.975	0.576	0.651	1.151	0	0.302	γ	2.302	2	−0.302
1.2	0.080	1.109	0.580	0.659	1.159	0	0.319		2.319	2	−0.319
1.4	0.084	1.242	0.584	0.667	1.167	0	0.335		2.335	2	−0.335
1.6	0.088	1.375	0.588	0.675	1.175	0	0.350		2.350	2	−0.350
1.8	0.091	1.509	0.591	0.682	1.182	0	0.365	↓	2.365	2	−0.365
2.0	0.095	1.642	0.595	0.689	1.189	0	0.379	1.189	2.379	2	−0.379

Case (c): Isotropic $\varepsilon = 1$, $\varepsilon_d = 0$

N	ν	γ	η	z	α
1	0.673	1.310	0.019	2.0135	0.108
2	0.722	1.400	0.020	2.0145	0.046
3	0.820	1.478	0.021	2.015	0.011

Case (d): Cubic anisotropic $\varepsilon = 1$, $\varepsilon_d = 0$

N	γ	η	z	α
3	1.222	0.021	2.015	0.244

[a] The extended ($\varepsilon_d > 0$) [pointlike ($\varepsilon_d = 0$)] defect XY systems for $\varepsilon = 1$ and $\varepsilon = 2$ are classified for (a) and (b), respectively. For comparison the isotropic and the cubic anisotropic systems are classified as (c) and (d), respectively, whose results were obtained by LeGuillou and Yamazaki, respectively. δ^*, φ, and the ($\nu_\perp$,..., α) stand for the fixed point value of δ, the crossover exponent for the randomness, and the critical exponents expressed in (4.16), (4.17), respectively. The values of ξ are equal to those of γ except for $\varepsilon_d = 0$.

the case of $\varepsilon_d = 2$ two-dimensional extended defect systems this model is not available simply because there are no magnetic atoms at all; (3) the regular-cubic-anisotropic fixed points are stable in the systems with $N \geqslant 3$. As we stand on the point of view of understanding the phase transitions and critical phenomena in various random systems due to the defects (including dislocations, disclinations, etc.), impurities and so on by introducing the fractal dimensions into the extended defect systems, we consider the cases of ε_d with nonnegative real numbers.

The characteristic features of extended defect systems may be summarized as follows:

(1) The effective strength of random defect interactions δ^* heightens with increasing ε_d and ε (i.e., decreasing d).

(2) The crossover exponent for randomness $\varphi = \alpha_p + \varepsilon_d \nu_p$ (α_p and ν_p stand for critical exponents α and ν for specific heat and correlation length of the corresponding regular systems) is positive, i.e., the randomness is relevant, and its values increase with increasing ε_d and ε.

(3) The values of $\nu_\perp$ (which corresponds to ν in the regular systems) and $\nu_\parallel$ become large with an increase of ε_d and ε, but they are small compared with those of the regular systems, i.e., they are near classical values (such features also appear in γ and ξ).

(4) Since $\nu_\parallel > \nu_\perp$ and $\eta_\parallel > \eta_\perp$ (except for $\varepsilon_d = 0$) and since they increase with increasing ε_d and ε, it mans that with an increase of ε_d, a short-range correlation develops more strongly in the parallel component and further in the two-dimensional systems, while the long-range correlation enlarges more rapidly in the parallel component near the critical point.

(5) The higher-order corrections modify the classical values of $\eta_\perp$ and $z_\parallel$.

(6) The dependences of $z_\perp$ on ε_d and ε are the same as those of γ, etc., while its magnitudes are larger than those of the regular systems.

(7) The values of α are negative, i.e., the specific heat does not display singular behavior.

From these features we may conclude the following:

(1) The randomness of the defect systems suppresses fluctuation effects and makes such behavior approach classical behavior.

(2) As the extended defects cut the interacting path of the spins perpendicular to the extended defect direction ($\parallel$), the short-range correlation strengthens and the long-range correlation develops more rapidly near the

transition point, compared to that in the perpendicular direction. That is, in the parallel direction the fluctuations are stronger and the correlation length more sharply divergent.

(3) As the defects randomly cut the path of the energy–energy correlation, the specific heat singularity does not appear.

(4) The values of the crossover exponent grow with an increase of magnitude of the defect's role, and are positive. That is, the randomness of the defects is relevant.

Finally the oscillating behavior of, e.g., the susceptibility of the D_{XY} systems, can be expressed by $\lambda = \lambda_R \pm i\lambda_I$ (λ_R, λ_I real) in (4.7), as

$$\chi^{-1} = c_1 t^{\gamma} \exp[c_2 t^{\lambda_R} \cos(\lambda_I \ln t + \theta) + c_3 t^{\lambda_c}]$$

where c_1, c_2, c_3, and θ are nonuniversal constants.

5. FIRST-ORDER PHASE TRANSITION

Stability arguments of the fixed points suggest that not only the continuous phase transition but also the discontinuous one appear, depending on the path of flow in the interaction space. Since the behavior of second-order phase transition was investigated in the previous section, here we take up first-order phase transition. Since the easy axes of the system D^c_{XY} consist of types $(\pm 1, 0)$ and $(0, \pm 1)$, the phase transfers from a state ordered uniaxially, e.g., along the x axis to the para-state.

The free energy of single-loop order is derived by (i) expressing bare free energy $[F_b \equiv F_0(M) + \frac{1}{2}\,\mathrm{Tr}\ln\{\delta^2 F_0/\delta\varphi_\alpha(x)\,\delta\varphi_\beta(y)|_{\varphi(x)=M}\}]$, (ii) renormalizing it using the replacement (3.1), (3.2), and applying the Taylor-expansion scheme around p^2 ($\equiv p_\perp^2 + a^2 p_\parallel^2$) for the integrands with respect to the internal momenta $\{p_\perp, p_\parallel\}$[i.e., $\ln(p^2+A) = \ln p^2 - A/p^2 + A^2/\{2p^2(p+q)^2\}|_{q^2=\kappa^2}$], and (iii) integrating over $\{p_\perp, p_\parallel\}$ after the change of variable $p_\parallel/a \to p_\parallel$. The dimensionless free energy expression is

$$\begin{aligned} F(\kappa) = {} & \tfrac{1}{2} t(\kappa)\, M^2(\kappa) + [g_s(\kappa) + g_c(\kappa) - 6\delta(\kappa)]\, M^4(\kappa)/4! \\ & + \tfrac{1}{8}[t(\kappa) + \{g_s(\kappa) + g_c(\kappa) - 6\delta(\kappa)\}\, M^2(\kappa)/2]^2 \\ & \times [[\ln[t(\kappa) + \{g_s(\kappa) + g_c(\kappa) - 6\delta(\kappa)\}\, M^2(\kappa)/2] + \tfrac{1}{2}]] \\ & + \tfrac{1}{8}[t(\kappa) + \{g_s(\kappa) - 6\delta(\kappa)\}\, M^2(\kappa)/6]^2 \\ & \times [[\ln[t(\kappa) + \{g_s(\kappa) - 6\delta(\kappa)\}\, M^2(\kappa)/6] + \tfrac{1}{2}]] \end{aligned} \tag{5.1}$$

where κ is the renormalization parameter and the free energy is expressed by $\kappa^{-d} a^{\epsilon_d} F(\kappa)$ with $\kappa = \kappa_\perp$.

The extremum of the free energy derives $M(\kappa)=0$ or the critical temperature $t(\kappa)$:

$$t(\kappa)=0 \quad \text{and} \quad t(\kappa)=\exp\{-1-2/[\tfrac{2}{3}g_s(\kappa)+\tfrac{1}{2}g_c(\kappa)-4\delta(\kappa)]\} \tag{5.2}$$

The thermodynamic stability can be given as

$$\partial^2 F(\kappa)/\partial M^2(\kappa)|_{M(\kappa)=0}=\tfrac{1}{2}\chi^{-1}(\kappa)$$
$$\chi^{-1}(\kappa)\equiv t(\kappa)[2+\tfrac{2}{3}g_s(\kappa)+\tfrac{1}{2}g_c(\kappa)-4\delta(\kappa)]\equiv t_c(\kappa)-t(\kappa) \tag{5.3}$$

The flow trajectory and thermodynamic stability for δ near null are illustrated in Fig. 3. The thermodynamically stable regions are enclosed by the marginal surfaces $2(g_s-6\delta)+g_c\geqslant 0$ and $g_s-6\delta+g_c\geqslant 0$. Choosing κ^*

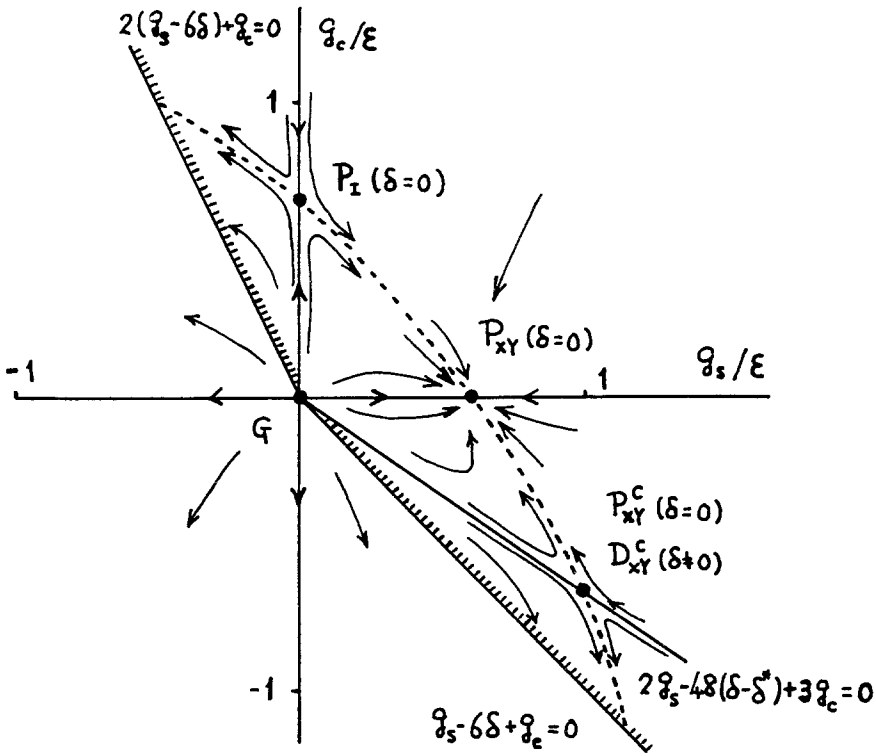

Fig. 3. Flow trajectory in the interaction space (g_s, g_c) near $\delta=0$. The shaded region denotes the thermodynamically stable region in the mean field theory. The principal trajectories connecting the fixed points are hatched by a dashed curve. The surfaces $g_s=0$ and $2g_s+3g_c-48(\delta-\delta^*)=0$ are the surface of the tricritical point.

at the edge of the stable region $g_s(\kappa^*) + g_c(\kappa^*) - 6\delta(\kappa^*) = 0$, we investigate the region

$$\begin{aligned} [g_s(\kappa^*) - 6\delta(\kappa^*)]/6 &\equiv A\varepsilon^{1/2} \\ g_s(\kappa^*) + g_c(\kappa^*) - 6\delta(\kappa^*) &\equiv B\varepsilon \qquad (B > 0) \\ t(\kappa^*) &\equiv b\varepsilon^{1/2}[\![\varepsilon]\!] \\ M^2(\kappa^*) &\equiv c\varepsilon^{-1/2}[\![\varepsilon^{-1}]\!] \end{aligned} \tag{5.4}$$

for the $D^c_{XY}[\![P^c_{XY}]\!]$ fixed point. The first-order phase transition takes place at the point where the free energy equals that of the para-state and becomes minimum with nonzero magnetization ($M \neq 0$):

$$\begin{aligned} b + \tfrac{1}{6}Bc + \tfrac{1}{2}A^2c[\ln(Ac) + 1] &= 0 \\ c[2b + \tfrac{1}{6}Bc + \tfrac{1}{2}A^2c\{\ln(Ac) + \tfrac{1}{2}\}] &= 0 \end{aligned} \tag{5.5}$$

Therefore we get the relations

$$b = \frac{1}{4}A^2c \qquad \text{and} \qquad c = \frac{1}{A}\exp\left[-\left(\frac{3}{2} + \frac{B}{3A^2}\right)\right] \tag{5.6}$$

The solution satisfying (5.6) is related to first-order phase transition appearing in the runaway flow region. Transition temperature and the jump of magnetization are calculated in two steps. In the first step, the temperature t^* and the magnetization M^* at the boundary κ^* are

$$\begin{aligned} t^* &= t(\kappa^*)\kappa^{*-2} = b\varepsilon^{1/2}[\![\varepsilon]\!] \\ M^{*2} &= M^2(\kappa^*)\kappa^{*2-\varepsilon}a^{-\varepsilon_d} = c\varepsilon^{-1/2}[\![\varepsilon^{-1}]\!] \end{aligned} \tag{5.7}$$

with the initial condition $t(1) = t$ and $M(1) = M$. These equations (5.7) relate t^* and M^* to the initial renormalized interactions $\{g^*\}$ and the dimensions $\{\varepsilon, \varepsilon_d\}$ via κ^*. In the second step, the flow equations for $t(\kappa)$ and $M(\kappa)$ are evaluated as

$$t(\kappa) = tf_t(\kappa), \qquad M(\kappa) = Mf_M(\kappa) \tag{5.8}$$

which are solved in Appendix B. At the first-order transition point, the temperature t_1 and the mgnetization M_1 are expressed as $t = t_1$ and $M = M_1$ in (5.8); therefore connecting (5.7) with (5.8), we get the transition temperature and the magnetization jump

$$t_1 = \frac{\kappa^{*2}}{f_t(\kappa^*)}b\varepsilon^{1/2}[\![\varepsilon]\!], \qquad M_1^2 = \frac{\kappa^{*2-\varepsilon}a^{-\varepsilon_d}}{f_M^2(\kappa^*)}c\varepsilon^{-1/2}[\![\varepsilon^{-1}]\!] \tag{5.9}$$

at the first-order transition point. Note that they also can be evaluated in terms of the values of κ^* and $\{g^*\}$.

In order to do so, the tricritical behavior of the system D^c_{XY} must be investigated. According to the tricritical hypothesis,[22] the singular part of the free energy of the systems near the tricritical point can be expressed as

$$F(t, \Delta, h) = g_t^{d/y_{tc}} \Phi(g_\Delta |g_t|^{-\phi_t}, g_h |g_t|^{-x_{tc}/y_{tc}}) \tag{5.10}$$

where y_{tc} ($\equiv d/(2-\alpha_{tc})$; α_{tc}: specific heat exponent) and x_{tc} stand for the Kadanoff temperature and magnetic-field-scaling parameters,[23] respectively. ϕ_t denotes the tricritical crossover exponent.[22] The nonlinear scaling fields for the tricritical parameter Δ (different parameter from bare defect interaction) and the mgnetic field h is denoted by g_Δ and g_t, respectively. The latter field is related to the relative temperature as

$$g_t \propto \begin{cases} (T - T_t)/T_t, & \Delta = 0 \\ [T - T_c(\Delta)]/T_c(\Delta), & \Delta < 0 \end{cases} \tag{5.11}$$

With the notations in Appendix B, the renormalized nonlinear scaling fields are expressed as

$$g_t(\kappa) = g_t \kappa^{-y_{tc}}, \qquad g_\Delta(\kappa) = g_\Delta \kappa^{-z_t}, \qquad g_h(\kappa) = g_h \kappa^{-x_{tc}} \tag{5.12}$$

From the results obtained in Section 4, the values of the critical exponents are

$$y_{tc} = 2 + O\{\varepsilon\}, \qquad z_t = 8\delta^* + O\{\varepsilon\}, \qquad x_{tc} = 3 + O\{\varepsilon\}$$
$$\phi_t = z_t / y_{tc} = 4\delta^* + O\{\varepsilon\} \tag{5.13}$$

where z_t means the propagation away from the unstable tricritical fixed point, which is derived from the respective eigenvalue. The scaling relations tell us that the first-order transition appears for $g_t \propto g_\Delta^{1/\phi_t} \propto g_\Delta^{1/(4\delta^*)}$, and that the jump of the magnetization ($M \propto -\partial F/\partial g_h$) is proportional to $g_\Delta^{(d-x_{tc})/\phi_t y_{tc}} \propto g_\Delta^{1/(8\delta^*)}$.

Using the results (B6) and (B1–B3), these nonlinear scaling fields were expressed:

$$g_\Delta(\kappa) = g_\Delta \kappa^{-\varepsilon z_\Delta} \equiv \{c_\Delta g_s(\kappa)[\mathscr{F}_c(\kappa) + \hat{\alpha}]^3 \mathscr{F}_c^{-2-\varepsilon_d/8}(\kappa)[\mathscr{F}_c(\kappa) + \hat{\beta}]^{-3+\varepsilon_d/8}\}^{z_\Delta} \tag{5.14.1}$$

$$c_\Delta \equiv \left[\frac{\hat{\alpha}^{2+\varepsilon_d/8}(-\hat{\alpha}+\hat{\beta})^{3-\varepsilon_d/8}}{24\delta^*}\right], \qquad z_\Delta \equiv 8 \cdot \delta^0 \varepsilon^{-1/2}, \qquad \delta^0 \equiv \left[\frac{3\tilde{\varepsilon}(3\tilde{\varepsilon}/\varepsilon - 2)}{8(353\tilde{\varepsilon} - 36\varepsilon)}\right]^{1/2}$$

$$g_t(\kappa) = g_t \kappa^{-y_{tc}} \equiv t(\kappa)[c_t \mathscr{F}_c^{-5/6+\varepsilon_d/24}(\kappa)|\mathscr{F}_c(\kappa) + \hat{\beta}|^{1/2-\varepsilon_d/24} g_s^{-1/3}(\kappa)]$$
$$= t(c_t \mathscr{F}_{c0}^{-5/6+\varepsilon_d/24}|\mathscr{F}_{c0} + \hat{\beta}|^{1/2-\varepsilon_d/24} g_s^{*-1/3}) \kappa^{-2+\varepsilon/3} \tag{5.14.2}$$
$$c_t \equiv \hat{\alpha}^{5/6-\varepsilon_d/24}|-\hat{\alpha}+\hat{\beta}|^{-1/2+\varepsilon_d/24} g_s^{*1/3}$$

where the factors $\{c_\Delta, c_t\}$ were chosen so as to satisfy $g_\Delta(\kappa) \to g_\Delta$ and $g_t(\kappa) \to t$ at the tricritical fixed point. In general, the renormalized interactions $\{g(\kappa)\}$ and temperature $t(\kappa)$ were represented by nonlinear scaling fields $\{g_\Delta(\kappa), g_t(\kappa)\}$ and the irrelevant nonlinear scaling field in (B7); however, for simplicity, the principal trajectory (B5.1) was considered. Here nonlinear scaling fields are described as

$$g_\Delta(\kappa) = \{(\varepsilon 2 c_\Delta)\, Y_1[\mathscr{F}_c(\kappa)][\mathscr{F}_c(\kappa) + \hat{\alpha}]^3\, \mathscr{F}_c^{-2-\varepsilon_d/8}(\kappa)\, |\mathscr{F}_c(\kappa) + \hat{\beta}|^{-3+\varepsilon_d/8}\}^{z_\Delta} \tag{5.15.1}$$

$$g_t(\kappa) = t(\kappa)[c_t(\varepsilon 2)^{-1/3}\, Y_1^{-1/3}[\mathscr{F}_c(\kappa)]\, \mathscr{F}_c^{-5/6+\varepsilon_d/24}(\kappa)\, |\mathscr{F}_c(\kappa) + \hat{\beta}|^{1/2-\varepsilon_d/24}] \tag{5.15.2}$$

Let us determine the value of κ^*. As the value of $\mathscr{F}_c(\kappa^*)$ becomes a complex number, introducing the shift $\mathscr{S}(<0)$ from the stability boundary as

$$\mathscr{F}_c(\kappa^*) + 1 + \mathscr{S} \equiv 6\mathscr{F}_\delta(\kappa^*), \qquad \text{i.e.,}\ B\varepsilon \equiv -\mathscr{S} g_s(\kappa^*) \tag{5.16}$$

gives a value of $\mathscr{S}$ for $\mathscr{F}_c(\kappa^*)$ real

$$\mathscr{S} \geqslant \{(5 \mp 2\sqrt{3}) - 4(3 \mp \sqrt{3})^{1/2}\}/\{2(3 \pm \sqrt{3})\} \equiv \mathscr{S}_\pm^* = \begin{cases} -0.3136 \\ -0.0935, \end{cases}$$

$$\text{i.e.,}\ -\mathscr{S}_-^* \leqslant -\mathscr{S} \leqslant -\mathscr{S}_+^* \tag{5.17}$$

where

$$\mathscr{F}_c^*(\kappa^*) = -[4 - (3 \mp \sqrt{3})^{1/2}]/[3 \pm \sqrt{3}] = \begin{cases} -0.0673 \\ -1.4391 \end{cases}$$

$$A^* \varepsilon^{1/2} = -[\mathscr{S}^* + \mathscr{F}_c^*(\kappa^*)]\, g_s(\kappa^*)/6 \tag{5.18}$$

Similarly we define the critical value $\mathscr{S}_\pm^*$

$$g_\Delta(\kappa^*) = g_\Delta \kappa^{*\varepsilon z_\Delta} \equiv g_\Delta^*, \qquad g_t(\kappa^*) = g_t \kappa^{*-y_{tc}} \equiv g_t^*, \qquad g_s(\kappa^*) \equiv \varepsilon 2 Y_1^* \tag{5.19}$$

and determine

$$\kappa^* = (g_\Delta / g_\Delta^*)^{1/(\varepsilon z_\Delta)} \tag{5.20}$$

Therefore the final expressions at the first-order transition point are obtained:

$$\begin{aligned} g_t = t_1 &= [\tfrac{1}{12} |\mathscr{S} + \mathscr{F}_c| \varepsilon Y_1\, e^{-(3/2 + B/3A^2)}]_*\, \hat{g}_t^*(g_\Delta/g_\Delta^*)^{2/(\varepsilon z_\Delta)} \\ \Delta M = M_1 &= [\sqrt{6}\{|\mathscr{S} + \mathscr{F}_c| \varepsilon 2 Y_1\}^{-1/2}\, e^{-(1/2)(3/2 + B/3A^2)}]_*\, (g_\Delta/g_\Delta^*)^{1/(\varepsilon z_\Delta)} \end{aligned} \tag{5.21}$$

where $\hat{g}_t^* \equiv g_t^*/t(\kappa^*)$ and $[\ ]_*$ stands for the value of $[\ ]$ at the critical value $\mathscr{S}^*$. Numerically we compare the values of free energy for the upper sign $(+)$ (which corresponds to $\hat{\beta} = 0.8453$) with those for the lower sign $(-)$ (which associates with $\hat{\beta} = 3.1547$). They are tabulated in Table II(a) and II(b) for the cases of $\varepsilon = 1$ and 2, respectively. These numerical results show that the free energy for the lower sign is most stable over the whole physical ranges of ε_d in the three- and two-dimensional systems. There the numerical expressions for the temperature shift and the magnetization jump are defined as

$$\begin{aligned} g_t &\equiv g_t^*(g_\Delta/g_\Delta^*)^{2/z_\Delta}, \qquad \Delta M \equiv \Delta M^*(g_\Delta/g_\Delta^*)^{1/z_\Delta} \\ g_\Delta^* &\equiv (c_\Delta^*)^{\hat{z}_\Delta}, \qquad \hat{z}_\Delta \equiv \{z_\Delta \text{ for (a) and (b), } 1/3 \text{ for (c)}\} \end{aligned} \tag{5.22}$$

Values for $\varepsilon = 1$ and 2 are tabulated in Table III(a) and III(b), respectively. For comparison, similar values for the cubic anisotropic XY system with $\varepsilon = 1$, 2 obtained by Rudnick[21] (in whose expressions 64/405 should be replaced by 68/405) are tabulated in Table III(c). The magnitudes of g_t increase (decrease) with increasing ε_d in the three-(two-) dimensional systems. In the pointlike defect systems they are approximately 20 (10) times those of the regular systems. The values of ΔM^* decrease with an increase of ε_d for $\varepsilon = 1$, 2, and with increasing ε for ε_d fixed. In the pointlike defect systems they are approximately $1/3 \sim 1/2$ of those of the regular systems. The exponent $1/z_\Delta$ decreases with increasing ε_d, while it increases with an increase of ε. The ε dependence of $\hat{z}_\Delta$ in the defect systems comes from the $\varepsilon^{1/2}$ expansion (notice that $\hat{z}_\Delta$ in the regular XY systems is independent of ε).

Table II. Comparison of the Free Energy Expressed in (5.1)[a]

ε_d \ $\hat{\beta}$	Case (a) $\varepsilon = 1$		Case (b) $\varepsilon = 2$	
	0.8453	3.1547	0.8453	3.1547
0	-0.286×10^{-4}	-0.276×10^{-3}	-0.126×10^{-2}	-0.485×10^{-2}
0.4	-0.214×10^{-4}	-0.362×10^{-3}	-0.109×10^{-2}	-0.540×10^{-2}
0.8	-0.156×10^{-4}	-0.448×10^{-3}	-0.941×10^{-3}	-0.587×10^{-2}
1.2	-0.110×10^{-4}	-0.534×10^{-3}	-0.797×10^{-3}	-0.630×10^{-2}
1.6	-0.750×10^{-5}	-0.619×10^{-3}	-0.664×10^{-3}	-0.668×10^{-2}
2.0	-0.489×10^{-5}	-0.703×10^{-3}	-0.541×10^{-3}	-0.704×10^{-2}

[a] The upper (lower) sign corresponds to $\hat{\beta} = 0.8453$ (3.1547). The numerical values show that the free energy on the trajectry for the lower sign is most stable in the extended- and the pointlike-defect XY systems in three and two dimensions.

Table III. Numerical Values Associated with the Behavior of the Temperature Shift and the Magnetization Jump at and near the First-Order Phase Transition Point[a,b]

ε_d \ Values	Case (a): $\varepsilon = 1$				Case (b): $\varepsilon = 2$			
	g_t^*	c_Δ^*	ΔM^*	$1/z_\Delta$	g_t^*	c_Δ^*	ΔM^*	$1/z_\Delta$
0	0.503	0.199	0.817	3.634	0.448	0.281	0.720	5.144
0.2	0.515	0.185	0.802	2.900	0.444	0.289	0.681	4.529
0.4	0.520	0.180	0.783	2.490	0.440	0.296	0.648	4.098
0.6	0.521	0.178	0.762	2.216	0.437	0.303	0.618	3.776
0.8	0.522	0.177	0.740	2.019	0.434	0.309	0.591	3.521
1.0	0.522	0.177	0.720	1.868	0.432	0.314	0.568	3.311
1.2	0.523	0.177	0.700	1.746	0.430	0.318	0.547	3.137
1.4	0.523	0.177	0.681	1.645	0.429	0.321	0.528	2.987
1.6	0.523	0.177	0.664	1.561	0.427	0.323	0.511	2.857
1.8	0.523	0.176	0.648	1.488	0.427	0.325	0.495	2.744
2.0	0.524	0.176	0.632	1.425	0.426	0.326	0.481	2.643
ε \ ε_d	Case (c): Cubic anisotropic							
	$\varepsilon = 1$				$\varepsilon = 2$			
0	0.026	0.168	2.389	3	0.052	0.168	1.689	1.5

[a] (a) and (b) are associated with the three- and two-dimensional extended ($\varepsilon_d > 0$) [pointlike ($\varepsilon_d = 0$)] defect *XY* systems, respectively. (c) corresponds to the regular cubic-anisotropic *XY* systems. The quantities ($g_t^*, \ldots, 1/z_\Delta$) are defined in footnote b. g_t^* and ΔM^* express the magnitudes of the temperature shift and the magnetization jump at the transition point, and $1/z_\Delta$ stands for their power law behavior.

[b] Note: $g_t = g_t^*(g_\Delta/g_\Delta^*)^{2/z_\Delta}$, $g_\Delta^* = (c_\Delta^*)^{z_\Delta}$, $\Delta M = \Delta M^*(g_\Delta/g_\Delta^*)^{1/z_\Delta}$, $\hat{z}_\Delta = \{z_\Delta$ for (a) and (b), 1/3 for (c)$\}$.

These results are available when $\{g_s(\kappa^*), g_c(\kappa^*), \delta(\kappa^*)\}$ approaches, not the fixed point, but the marginal boundary of the stable regime. If the set of interactions approach the D_{XY}^c fixed point inside the stable region, it causes a second-order phase transition. Therefore, the surface $2g_s + 3g_c - 48(\delta - \delta^*) = 0$ is a surface of tricritical points. When the set of interactions $\{g(\kappa^*)\}$ lie close to, but below the plane, there exist regions satisfying (5.4), i.e., a first-order phase transition (5.22).

6. CONCLUSION

The static and dynamic critical behavior of extended defect *XY*-spin systems in cubic anisotropic crystallines were investigated. Applying the

field-theoretic RG approach together with a $\varepsilon^{1/2}$-type or ε-type expansion, the static and dynamic behavior was evaluated up to two-loop order within the frame of the Langevin equation. Results were obtained for (i) fixed points, (ii) fixed point stability, (iii) flow trajectory, (iv) static and dynamic critical exponents for perpendicular and parallel components on the trajectory of the second-order phase transition, and (v) behavior of the first-order phase transition near the tricritical point.

As mentioned above, fixed points (i)–(vii) have been previously investigated. Fixed point (viii), reported here for the first time, belongs to the $\varepsilon^{1/2}$-type expanded systems. It displays a most interesting cooperative or competitive effect between cubic anisotropy and random defect interaction.

Let us consider the reasons. The $\varepsilon^{1/2}$-type expansion originates in situations where the $\{\beta\}$ functions in the RG equations are degenerate in single-loop order but solved in two-loop order. Why do such situations occur in the Ising systems for (vii) or in the XY-spin systems for (viii)? In the first case, it is the fact that, in single-loop order, the β_s function for the isotropic interaction g_s of the N-component systems has only for $N=1$ the same gradient as that of the β_δ function for the random defect interaction δ in the space (g_s, δ), and the fact that their gradients become unequal due to the nonlinearity in the two-loop order contributions. Furthermore, the interaction δ is regarded as unit vector in the space (g_s, δ), i.e., as single component in the spin space. In the second case the gradients of the β_c and β_δ functions become the same for $N=2$ in space (g_s, g_c, δ) in single-loop order and their gradients become different in two-loop order. Furthermore, the interactions g_c and δ are individually regarded as single components in the spin space, and they behave totally as two-component spins. This clearly indicates cooperative phenomena among interactions g_s, g_c, and δ. Thus there is high probability of finding such systems with other components, e.g., $N=3$, 4, 5,... studied under $\varepsilon^{1/2}$-type expansion. Presumably, there are also similar possibilities with systems utilizing the $\varepsilon^{1/3}, \varepsilon^{1/4}$,..., expansions. There we may expect that the β functions in the RG equations are degenerate up to two (three,...,)-loop order for $\varepsilon^{1/3}$ ($\varepsilon^{1/4}$,...,) expansion and become nondegenerate in the next-higher loop order.

According to results obtained on fixed point stability, the system P_{XY} is most stable as regular systems, but with the appearance of defects the extended defect system D_{XY} becomes most stable. This fixed point has quite interesting properties, i.e., its flow trajectories in the interaction space approach the fixed point D_{XY}, monotonically (nonoscillatorily) in a small value of $0 \leqslant \varepsilon_d/\varepsilon < 0.02733$ but spirally in a large value of $0.02733 < \varepsilon_d/\varepsilon$. The other fixed points are unstable in certain directions of the interaction space, i.e., their flow trajectories suggest first-order phase transition.

Regarding the trajectory of second-order phase transition (i.e., flows

heading toward fixed point D_{XY}^c with an increase of the correlation length), the values of the static and dynamic critical exponents $\{\varphi, \nu_\perp, \nu_\parallel, \gamma, \eta_\perp, \eta_\parallel, \xi, z_\perp, z_\parallel, \alpha\}$ of order $\varepsilon^{1/2}$ were evaluated and ε_d was considered as a nonnegative real number. The crossover exponent for randomness ($\varphi = \alpha_p + \varepsilon_d \nu_p$) is positive, i.e., the randomness of the defects is relevant in *XY* systems. Its value increases with an increase of ε_d and ε. Pointlike and extended defects play a role in cutting the path of the spin–spin or the energy–energy correlation. As a result, the effective medium dimension seems to be reduced, and the short-range correlation becomes strong, while the long-range correlation (fluctuation effect) is weakened. That is, the critical exponents approach classical values. These tendencies are stronger in the perpendicular component than in the parallel component. Comparing these critical exponent values with those obtained by Lawrie *et al.*[12] in the Ising systems without cubic anisotropy, the static and dynamic critical behavior of the present systems appear more readily available because the fluctuations of the order parameters are suppressed by the cubic anisotropy.

Regarding flows emanating from the fixed point D_{XY}^c: such flows are not attracted by any other fixed point, and are of first-order phase transition. The first-order transition occurs as a transition from the uniaxially ordered state to the para-state, due to cubic anisotropy. The crucial differences between extended defect *XY* systems with cubic anisotropy and the regular *XY* system with cubic anisotropy are derived from the defect interaction δ, the extended defect dimensions ε_d, and the $\varepsilon^{1/2}$ expansion. The main features here are as follows:

(1) A transition point for the real values of $\mathscr{F}_c$ shifts by $-\mathscr{S}$ (satisfying $-\mathscr{S}_-^* \leqslant -\mathscr{S} \leqslant -\mathscr{S}_+^*$) from the marginal boundary.

(2) The systems take the lowest free energy at point $\mathscr{S}_-^*$.

(3) At the transition point, the temperature shift g_t^* in the three-(two-) dimensional systems increases (decreases) with increasing ε_d, and the magnetization-jump ΔM^* in both dimensional systems decreases with an increase of ε_d.

(4) Near the transition point, behavior is expressed with the exponent $1/z_\Delta$ whose values decrease (increase) with increasing $\varepsilon_d(\varepsilon)$.

Finally a comment on defect effects in two-component systems. In the present systems, the primary role of cubic anisotropy is in first-order transition as well as in the regular cubic–anisotropic *XY* system, and the cooperation between the defect interaction and the cubic–anisotropic interaction yields a $\varepsilon^{1/2}$ expansion. This transition belongs to fluctuation-induced first-order transition. On the other hand, phase transition in the

superconductors is weakly first order due to the long-range effects of the electromagnetic field, according to the study by Halperin *et al.*[24]; this conclusion for type-II superconductors is based on the runaway behavior of the RG trajectories, calculated within the $4-\varepsilon$ expansion, which is consistent with calculations by Coleman *et al.*[25] and Lawrie.[26] However, in superconductors with quenched random defects (paramagnetic impurities), the phase transition becomes second order within the $4-\varepsilon$ expansion, according to Boyanovsky *et al.*[27]

In conclusion: (1) defect effects restore a second order of phase transition; (2) the ε-expansion form does not change into a $\varepsilon^{1/2}$ expansion; (3) at the fixed point the eigenvalues consist of one positive real and two complex eigenvalues, i.e., the RG trajectories spiral into the fixed point and give oscillatory corrections to scaling. This feature is also seen in the extended defect XY systems D_{XY}.

ACKNOWLEDGMENTS

Y. Y. wishes to express his gratitude to Profs. S. Katsura and S. Inawashiro for their encouragement and to Sonderforschungs-Bereich Ferroelektrika 130, Universität des Saarlandes, FRG, for two months support of this project. Further suport came from the Japanese Government (Ippan Kenkyu C).

APPENDIX A. DIAGRAMS AND CONTRIBUTIONS

Diagrams and contributions for $\Gamma^{(1,1)}$ are listed, respectively, in Fig. A1 and Table AI;

Table AI

Class of diagram \ Contributions	$\Gamma^{(1,1)}\big\|_{p^2=\omega=0}$	$\dfrac{\partial\Gamma^{(1,1)}}{\partial p_\perp^2}\Big\|_{p^2=\omega=0}$	$\dfrac{\partial\Gamma^{(1,1)}}{\partial p_\parallel^2}\Big\|_{p^2=\omega=0}$	$\dfrac{i\partial\Gamma^{(1,1)}}{\partial\omega}\Big\|_{p^2=\omega=0}$
(1.1), (1.2)	$-1/\varepsilon$	0	0	0
(2)	$-1/\tilde{\varepsilon}$	0	$a^2\tilde{\varepsilon}\tilde{I}_1$	$\tilde{\varepsilon}\tilde{I}_1$
(3.1)–(3.4)	I_1	0	0	0
(4.1)–(4.3)	I_2	I_3	$a^2 I_3$	I_4
(5.1), (5.2)	$\tilde{\varepsilon}\tilde{I}_1/\varepsilon$	0	0	0
(6.1), (6.2)	$2\tilde{\varepsilon}\tilde{I}_1/(\varepsilon+\tilde{\varepsilon})$	0	0	0
(7.1), (7.2)	J_1	J_2	$a^2 J_3$	J_3
(8)	$\tilde{I}_1$	0	$a^2 J_5$	J_5
(9)	$\tilde{I}_2$	$\tilde{I}_3$	$a^2 3\tilde{I}_1/2$	$3\tilde{I}_1/2$

In Table AI

$$I_1 \equiv -\frac{1}{\varepsilon^2}\left(1-\frac{\varepsilon}{2}\right), \qquad I_2 \equiv \frac{-3}{2\varepsilon^2}\left(1+\frac{\varepsilon}{2}\right)$$

$$I_3 = -\frac{1}{8\varepsilon}, \qquad I_4 \equiv -\frac{3}{4\varepsilon}\ln\frac{4}{3}$$

$$\tilde{I}_1 \equiv -\frac{1}{\tilde{\varepsilon}^2}\left(1-\frac{\tilde{\varepsilon}}{2}\right), \qquad \tilde{I}_2 \equiv -\frac{3}{2\tilde{\varepsilon}^2}\left(1+\frac{\tilde{\varepsilon}}{2}\right), \qquad \tilde{I}_3 \equiv -\frac{1}{8\tilde{\varepsilon}}$$

$$J_1 \equiv \frac{-(2\varepsilon+\tilde{\varepsilon}+3\varepsilon\tilde{\varepsilon}/2)}{\varepsilon\tilde{\varepsilon}(\varepsilon+\tilde{\varepsilon})}, \qquad J_2 \equiv -\frac{1}{4(\varepsilon+\tilde{\varepsilon})}, \qquad J_3 \equiv -\frac{(1-\tilde{\varepsilon}/2)}{\varepsilon(\varepsilon+\tilde{\varepsilon})}$$

$$J_5 \equiv \frac{-[1-(3/2)\tilde{\varepsilon}]}{\tilde{\varepsilon}^2}$$

Diagrams and contributions for $\Gamma^{(1,3)}_{g_s} - \Gamma^{(1,3)}_{g_c}$ are listed, respectively, in Fig. A2(a), and Table AII(a); diagrams and contributions for $\Gamma^{(2,2)}_{\delta}$ are listed, respectively, in Fig. A2(b) and Table AII(b).

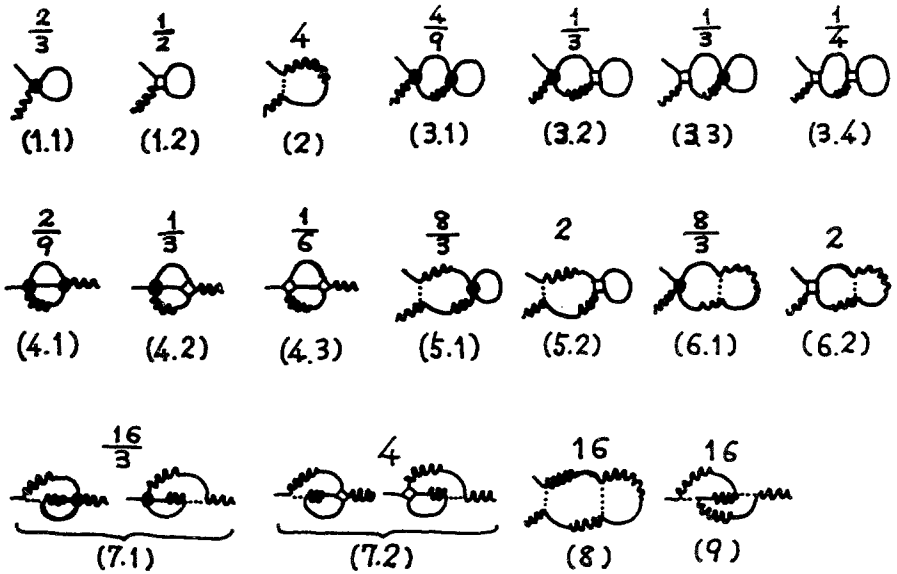

Fig. A1. Diagrams contributing to the $\Gamma^{(1,1)}$ vertex function. The number on the diagrams stands for the number of diagrams (weight). The symbols ●, □, and • • • are associated with the g_s, g_c, and δ interactions, respectively. The lines ~~~ and —— correspond to the response and correlation lines, respectively.

Table AII

Class of diagram		
Case (a)	Case (b)	Contribution
(1.1), (1.2)	(3.1), (3.2)	I_a
(2)	(1), (2)	$\tilde{I}_a$
(3.1)–(3.5)	(4.1)–(4.4), (5.1)–(5.3)	I_a^2
(7.1)–(7.3)	(7.1), (7.2), (8.1), (8.2)	$I_a\tilde{I}_a$
(4), (5)	(14), (15), (16)	$\tilde{I}_a^2$
(8.1), (8.2)	(6.1), (6.2)	I_b
(10.1)–(10.5)	(9.1)–(9.3)	I_c
(6), (13), (14)	(17), (18), (19), (20), (21)	$\tilde{I}_c$
(11.1)–(11.3)	(10.1), (10.2), (12.1), (12.2)	I_d
(9.1), (9.2), (12.1)–(12.3)	(11.1), (11.2), (13.1), (13.2)	$\tilde{I}_d$
(15.1), (15.2)		I_e
(16)	(22), (23)	I_f
	(24.1), (24.2)	$4I_e$

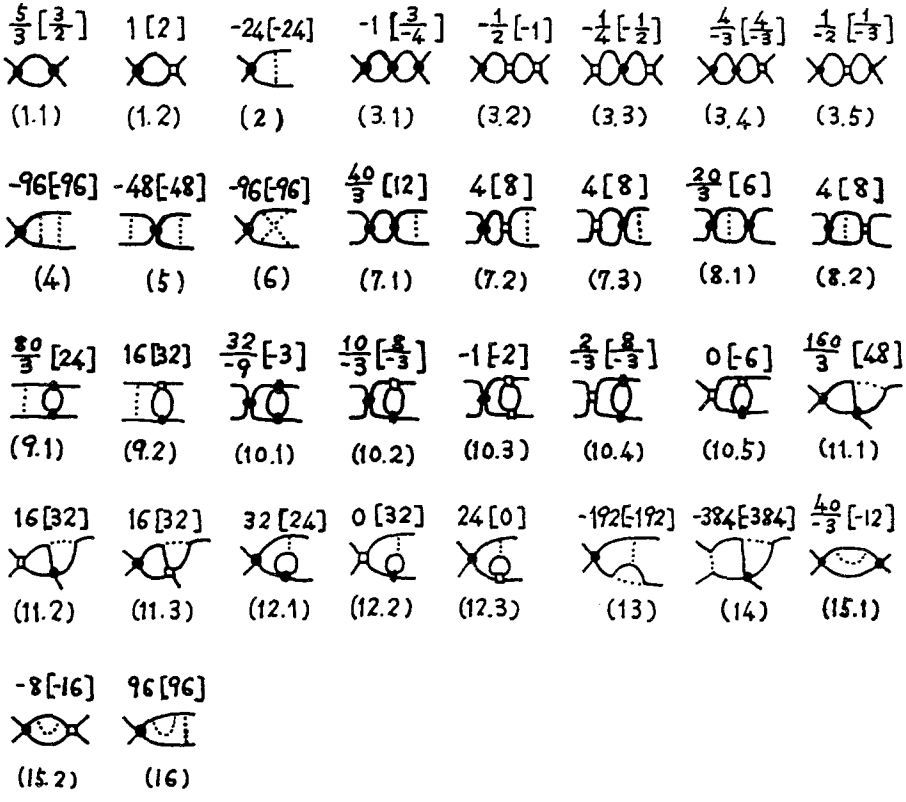

Fig. A2. (a) Diagrams contributing to the $\Gamma_{g_s}^{(1,3)}$ and $\Gamma_{g_c}^{(1,3)}$ vertex functions. The diagrams are drawn in the static case in order to decrease the number of diagrams. The first and the second (inside [ ]) numbers on the diagrams denote the weight of the diagrams for the $\Gamma_{g_s}^{(1,3)}$ and

In Table AII

$$I_a \equiv \frac{1}{\varepsilon}\left(1-\frac{\varepsilon}{2}\right), \qquad \tilde{I}_a \equiv \frac{1}{\tilde{\varepsilon}}\left(1-\frac{\tilde{\varepsilon}}{2}\right), \qquad I_b \equiv \frac{2}{\tilde{\varepsilon}(\varepsilon+\tilde{\varepsilon})}\left(1-\frac{\varepsilon+\tilde{\varepsilon}}{2}\right)$$

$$I_c \equiv \frac{1}{2\varepsilon^2}\left(1-\frac{\varepsilon}{2}\right), \qquad \tilde{I}_c \equiv \frac{1}{2\tilde{\varepsilon}^2}\left(1-\frac{\tilde{\varepsilon}}{2}\right), \qquad I_d \equiv \frac{1}{\tilde{\varepsilon}(\varepsilon+\tilde{\varepsilon})}\left(1-\frac{\varepsilon}{2}\right)$$

$$\tilde{I}_d \equiv \frac{1}{\varepsilon(\varepsilon+\tilde{\varepsilon})}\left(1-\frac{\tilde{\varepsilon}}{2}\right), \qquad I_e \equiv \frac{\varepsilon_d}{4\tilde{\varepsilon}(\varepsilon+\tilde{\varepsilon})}$$

$$I_f \equiv \frac{1}{\tilde{\varepsilon}}\left[\int \frac{d^d q (a^2 p_\parallel^2)^{1-\tilde{\varepsilon}/2}}{(q_\perp^2 + a^2 p_\parallel^2)^2 [(q_\perp - \kappa_\perp)^2 + a^2 s_\parallel^2]} + (\text{permutation of } p_\parallel \to s_\parallel)\right]$$

Here the contributions of the integrals of the logarithmic terms are omitted for simplicity.

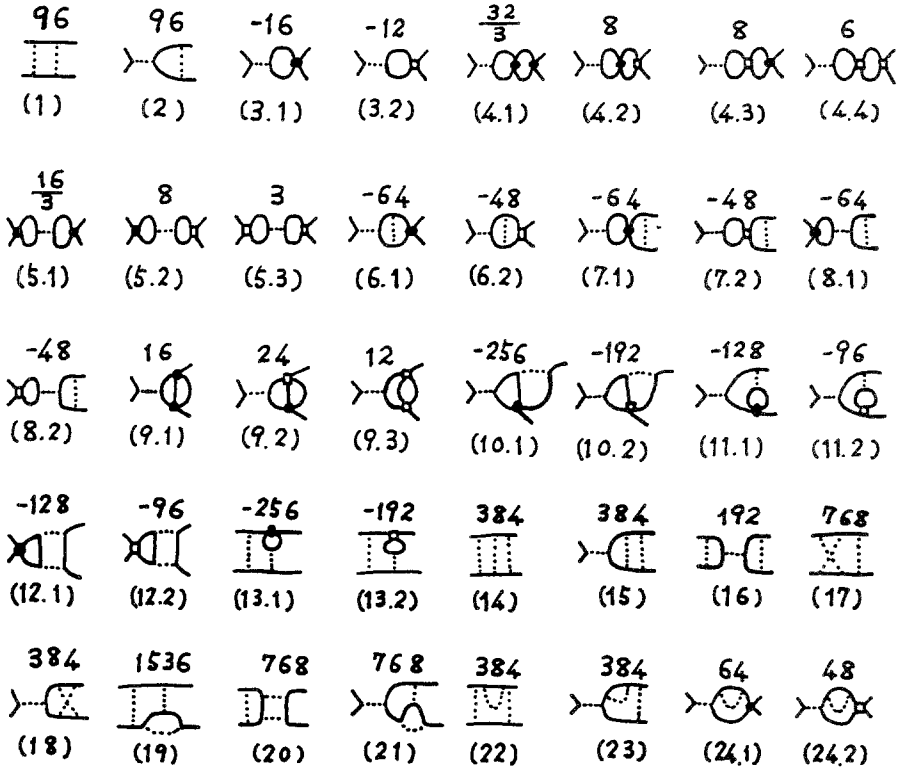

$\Gamma_{g_c}^{(1,3)}$ vertex functions, respectively. The number inside [ ] in the cases of ( ) or (α, 1) for $\alpha = 1,\ldots, 15$ corresponds to that obtained by replacing the interaction g_s with g_c. (b) Diagrams contributing to the $\Gamma_\delta^{(2,2)}$ vertex function. These diagrams are drawn in the static limit and the number on the diagrams stands for weight.

822/41/3-4-12

APPENDIX B. FLOW OF RENORMALIZED INTERACTIONS

A study of the flow of renormalized interactions $\{g(\kappa)\}$ depending on the renormalization parameter κ by means of the characteristic curve method. Change variables in (4.1)

$$g_s(\kappa, a) \equiv G_s(\kappa, a)\, xy, \qquad g_c(\kappa, a) \equiv G_c(\kappa, a)\, xy, \qquad \delta(\kappa, a) \equiv G_\delta(\kappa, a)\tilde{x}$$

$$x \equiv \kappa_\perp^{-\varepsilon}, \qquad y \equiv a^{-\varepsilon_d}, \qquad \tilde{x} \equiv \kappa_\perp^{-\tilde{\varepsilon}}, \qquad [a] \equiv [\kappa_\perp/\kappa_\parallel], \qquad \tilde{\varepsilon} \equiv \varepsilon + \varepsilon_d$$

and introduce the new variables

$$\mathscr{F}_c(G_s) \equiv g_c(\kappa, a)/g_s(\kappa, a), \qquad \mathscr{F}_\delta(G_s) \equiv \delta(\kappa, a)/g_s(\kappa, a)$$

if necessary. Regard $\kappa_\perp$ as κ, and the dimensions of xy equal those of $\tilde{x}$ in the unit of κ. For the sake of simplicity, consider the case $xy = \tilde{x}$. Then the renormalized flow (characteristic curve) equations, which determine the renormalized interactions, temperature, and coordinate anisotropy, are expressed from (4.1) and (4.2) by the differential equations

$$-\varepsilon \frac{dG_s}{dx} = \left(\frac{5}{3} + \mathscr{F}_c - 24\mathscr{F}_\delta\right) G_s^2\, y$$

$$-\varepsilon \frac{d(G_s\mathscr{F}_c)}{dx} = \left(2 + \frac{3}{2}\mathscr{F}_c - 24\mathscr{F}_\delta\right) \mathscr{F}_c G_s^2\, y$$

$$-\varepsilon \frac{d(G_s\mathscr{F}_\delta)}{dx} = \left(\frac{4}{3} + \mathscr{F}_c - 16\mathscr{F}_\delta\right) \mathscr{F}_\delta G_s^2\, y$$

$$-\varepsilon \frac{d \ln \kappa^2 t(\kappa)}{dx} = \left(\frac{2}{3} + \frac{1}{2}\mathscr{F}_c - 4\mathscr{F}_\delta\right) G_s\, y$$

$$-\varepsilon \frac{dy}{dx} = \varepsilon_d \mathscr{F}_\delta G_s\, y^2$$

with the initial conditions

$$G_s(1) = g_s, \qquad G_c(1) = g_c, \qquad G_\delta(1) = \delta, \qquad t(1) = t, \qquad y(1) = 1$$

The solutions for these equations give the following flow relations:

(ii) P_{XY} case on the $g_c = 0 = \delta$ line,

$$G_s(\kappa) = \frac{g_s}{[5(x-1)/3\varepsilon]\, g_s + 1}, \qquad t(\kappa) = \kappa^{-2} t \left[\frac{5(x-1)}{3\varepsilon}\, g_s + 1\right]^{-2/5}$$

(iii) P_I case on the $g_s = 0 = \delta$ line,

$$G_c(\kappa) = \frac{g_c}{[3(x-1)/2\varepsilon]\, g_c + 1}, \qquad t(\kappa) = \kappa^{-2} t \left[\frac{3(x-1)}{2\varepsilon} g_c + 1 \right]^{-1/3}$$

(iv) U case on the $g_s = 0 = g_c$ line,

$$G_\delta(\kappa) = \frac{\delta}{[1 - (x-1)/\varepsilon \cdot (1 - \varepsilon_d/16)\, 16\delta]^{1/(1-\varepsilon_d/16)}}$$

$$t(\kappa) = \kappa^{-2} t \left[1 - \frac{x-1}{\varepsilon} \left(1 - \frac{\varepsilon_d}{16} \right) 16\delta \right]^{-1/[4(1-\varepsilon_d/16)]}$$

(v) P^c_{XY} case on the $\delta = 0$ plane,

$$G_s(\mathscr{F}_c) = g_s \left(\frac{\mathscr{F}_c}{\mathscr{F}_{c0}} \right)^5 \left(\frac{\mathscr{F}_{c0} + 2/3}{\mathscr{F}_c + 2/3} \right)^3, \qquad t(\kappa) = \kappa^{-2} t \left(\frac{\mathscr{F}_c}{\mathscr{F}_{c0}} \right)^2 \left(\frac{\mathscr{F}_{c0} + 2/3}{\mathscr{F}_c + 2/3} \right)$$

$$\frac{x-1}{\varepsilon} = \frac{2}{g_s} \frac{\mathscr{F}_{c0}^5}{(\mathscr{F}_{c0} + 2/3)^3} [X_5(\mathscr{F}_c) - X_5(\mathscr{F}_{c0})],$$

$$X_5(\mathscr{F}) \equiv [\mathscr{F}^2/3 + \mathscr{F}/3 + 4/45]/\mathscr{F}^5$$

(vi) D_{XY} case on the $g_c = 0$ plane,

$$G_s(\mathscr{F}_\delta) = g_s \left(\frac{\mathscr{F}_{\delta 0}}{\mathscr{F}_\delta} \right)^5 \left(\frac{\mathscr{F}_\delta - 1/24}{\mathscr{F}_{\delta 0} - 1/24} \right)^2, \qquad t(\kappa) = \kappa^{-2} t \left(\frac{\mathscr{F}_{\delta 0}}{\mathscr{F}_\delta} \right)^2 \left(\frac{\mathscr{F}_\delta - 1/24}{\mathscr{F}_{\delta 0} - 1/24} \right)^{3/2}$$

$$y = \left(\frac{\mathscr{F}_\delta - 1/24}{\mathscr{F}_{\delta 0} - 1/24} \right)^{\varepsilon_d/8}, \qquad \frac{x-1}{\varepsilon} = \frac{(\mathscr{F}_{\delta 0} - 1/24)^{2+\varepsilon_d/8}}{8 g_s (\mathscr{F}_{\delta 0})^5} [X_6(\mathscr{F}_\delta) - X_6(\mathscr{F}_{\delta 0})]$$

$$X_6(\mathscr{F}) \equiv -\frac{\Gamma(5)}{\Gamma(3+\varepsilon_d/8)} \left[\sum_{i=0}^{2} \frac{\Gamma(2+\varepsilon_d/8-i)}{\Gamma(5-i)} \mathscr{F}^{4-i} \left(\mathscr{F} - \frac{1}{24} \right)^{-(2+\varepsilon_d/8-i)} \right.$$

$$\left. + \sum_{j=1}^{2} \frac{(-1)^j}{\Gamma(1-\varepsilon_d/8+j)} \mathscr{F}^{(2-j)} \left(\mathscr{F} - \frac{1}{24} \right)^{(j-\varepsilon_d/8)} \right]$$

(vii) D_I case on the $g_s = 0$ plane,

$$G_c(\mathscr{F}_\delta) = g_c \left(\frac{\mathscr{F}_{\delta 0}}{\mathscr{F}_\delta} \right)^3, \qquad t(\kappa) = \kappa^{-2} t \left(\frac{\mathscr{F}_{\delta 0}}{\mathscr{F}_\delta} \right) \left(\frac{\mathscr{F}_\delta - 1/16}{\mathscr{F}_{\delta 0} - 1/16} \right)^{1/2}$$

$$y = \left(\frac{\mathscr{F}_\delta - 1/16}{\mathscr{F}_{\delta 0} - 1/16} \right)^{\varepsilon_d/8}, \qquad \frac{x-1}{\varepsilon} = \frac{(\mathscr{F}_{\delta 0} - 1/16)^{\varepsilon_d/8}}{8 g_c (\mathscr{F}_{\delta 0})^3} [X_7(\mathscr{F}_\delta) - X_7(\mathscr{F}_{\delta 0})]$$

$$X_7(\mathscr{F}) \equiv -\frac{1}{a_2} \left(\mathscr{F} - \frac{1}{16} \right)^{a_2} - \frac{1}{8a_1} \left(\mathscr{F} - \frac{1}{16} \right)^{a_1} - \frac{1}{16^2 a_0} \left(\mathscr{F} - \frac{1}{16} \right)^{a_0}$$

$$a_2 \equiv 2 - \varepsilon_d/8, \qquad a_1 \equiv 1 - \varepsilon_d/8, \qquad a_0 \equiv -\varepsilon_d/8$$

(viii) D^{c}_{XY} case

$$\mathscr{F}_\delta \equiv \frac{1}{24}\left[1-\frac{1+2/3\mathscr{F}_{c0}}{1+2/3\mathscr{F}_c}\left(1-\frac{1}{24\mathscr{F}_{\delta 0}}\right)\right]^{-1}$$

$$G_s(\mathscr{F}_c) = g_s\left(\frac{\mathscr{F}_c}{\mathscr{F}_{c0}}\right)^2\left(\frac{\mathscr{F}_{c0}+\hat{\alpha}}{\mathscr{F}_c+\hat{\alpha}}\frac{\mathscr{F}_c+\hat{\beta}}{\mathscr{F}_{c0}+\hat{\beta}}\right)^3 \tag{B1}$$

$$t(\kappa) = \kappa^{-2}t\left(\frac{\mathscr{F}_c}{\mathscr{F}_{c0}}\right)^{3/2}\left(\frac{\mathscr{F}_{c0}+\hat{\alpha}}{\mathscr{F}_c+\hat{\alpha}}\right)\left(\frac{\mathscr{F}_c+\hat{\beta}}{\mathscr{F}_{c0}+\hat{\beta}}\right)^{1/2}, \qquad y = \left(\frac{\mathscr{F}_c}{\mathscr{F}_{c0}}\frac{\mathscr{F}_{c0}+\hat{\beta}}{\mathscr{F}_c+\hat{\beta}}\right)^{\varepsilon_d/8} \tag{B2}$$

$$\frac{x-1}{\varepsilon} = \frac{2}{g_s}\frac{(\mathscr{F}_{c0})^{2+\varepsilon_d/8}(\mathscr{F}_{c0}+\hat{\beta})^{3-\varepsilon_d/8}}{(\mathscr{F}_{c0}+\hat{\alpha})^3}\left[X_8(\mathscr{F}_c)-X_8(\mathscr{F}_{c0})\right]$$

$$X_8(\mathscr{F}) \equiv \int^{\mathscr{F}} \frac{(W+\hat{\alpha})^2\,dW}{(W)^{3+\varepsilon_d/8}(W+\hat{\beta})^{3-\varepsilon_d/8}} \tag{B3}$$

where

$$\hat{\alpha} \equiv 2/3, \qquad 1-\hat{\alpha}/\hat{\beta} \equiv [1+2/(3\mathscr{F}_{c0})][1-1/(24\mathscr{F}_{\delta 0})] \tag{B4}$$

and the subscript 0 denotes the initial value, e.g., $\mathscr{F}_{c0} = \mathscr{F}_c(1)$.

To derive the principal trajectory connecting the fixed points, after the cumbersome calculations we can express (B3) like

$$x-1 = \frac{\varepsilon 2}{g_s}\frac{(\mathscr{F}_{c0})^{2+\varepsilon_d/8}(\mathscr{F}_{c0}+\hat{\beta})^{3-\varepsilon_d/8}}{(\mathscr{F}_{c0}+\hat{\alpha})^3} \times \left\{\left[Y_j(w)\frac{(w+\hat{\alpha})^3}{(w)^{2+\varepsilon_d/8}(w+\hat{\beta})^{3-\varepsilon_d/8}}\right]\Bigg|_{w=\mathscr{F}_{c0}}^{\mathscr{F}_c}\right\} \qquad \text{for} \quad j=1,2 \tag{B5}$$

$$Y_1(w) \equiv \left[\mp\sqrt{3}\hat{\beta}^{-3}\left(w+\frac{1\mp\sqrt{3}}{2}\hat{\beta}\right)-\frac{\varepsilon_d}{8}\frac{3}{2}\hat{\beta}^{-3}(4\mp 3\sqrt{3}) \times \left(w-\frac{3\pm 5\sqrt{3}}{66}\hat{\beta}\right)\right](w+\hat{\beta})\left(\frac{w+\hat{\beta}}{w}\right)^{\varepsilon_d/8} \qquad \text{for} \quad \hat{\alpha}/\hat{\beta} = (3\pm\sqrt{3})/6 \tag{B5.1}$$

$$Y_2(w) \equiv \left[\sum_{i=0}^{3}\left(\frac{A_i}{2}+\frac{\varepsilon_d}{8}\frac{B_i}{4}\right)w^i\right](w+\hat{\beta})/(w+\hat{\alpha})^3 \qquad \text{for} \quad a_1 = 0 \tag{B5.2}$$

$$a_1 \equiv (\hat{\beta}^2-6\hat{\alpha}\hat{\beta}+6\hat{\alpha}^2)/\hat{\beta}^5, \qquad A_0 \equiv \hat{\alpha}^2/\hat{\beta}, \qquad A_1 \equiv 4\hat{\alpha}(\hat{\beta}-\hat{\alpha})/\hat{\beta}^2$$

$$A_2 \equiv -3(\hat{\beta}^2-6\hat{\alpha}\hat{\beta}+6\hat{\alpha}^2)/\hat{\beta}^3, \qquad A_3 \equiv -2(\hat{\beta}^2-6\hat{\alpha}\hat{\beta}+6\hat{\alpha}^2)/\hat{\beta}^4$$

$$B_0 = -\hat{\alpha}^2/\hat{\beta}, \qquad B_1 \equiv -4(2\hat{\beta}-3\hat{\alpha})\hat{\alpha}/\hat{\beta}^2$$

$$B_2 \equiv -(7\hat{\beta}^2-6\hat{\alpha}\hat{\beta}-12\hat{\alpha}^2)/\hat{\beta}^3, \qquad B_3 \equiv -6(\hat{\beta}-2\hat{\alpha})/\hat{\beta}^3$$

where the expression for Y_1 is available only when the initial values of $\mathscr{F}_{c0}$ and $\mathscr{F}_{\delta 0}$ are chosen so as to satisfy $\hat{\alpha}/\hat{\beta} = (3 \pm \sqrt{3})/6$, and then Y_2 holds also because $a_1 = 0$. Substituting (B5), $G_s(\kappa)$, and y into $g_s(\kappa) = G_s(\kappa)\, xy$, we can derive the relations

$$\frac{\mathscr{F}_c^{2+\varepsilon_d/8}(\mathscr{F}_c + \hat{\beta})^{3-\varepsilon_d/8}}{(\mathscr{F}_c + \hat{\alpha})^3} \frac{1}{g_s(\kappa)} = \frac{\mathscr{F}_{c0}^{2+\varepsilon_d/8}(\mathscr{F}_{c0} + \hat{\beta})^{3-\varepsilon_d/8}}{(\mathscr{F}_{c0} + \hat{\alpha})^3} \frac{1}{g_s x} \tag{B6}$$

$$[1 - \varepsilon 2 Y_j(\mathscr{F}_c)/g_s(\kappa)] = [1 - \varepsilon 2 Y_j(\mathscr{F}_{c0})/g_s] \frac{1}{x} \qquad \text{for} \quad j = 1, 2 \tag{B7}$$

The first expression is associated with the nonlinear scaling field $g_4(\kappa)$ described in Section 5. The second relations are connected with the two principal trajectories

$$g_s = \varepsilon 2 Y_1(\mathscr{F}_c) \tag{B8}$$

and

$$g_c = \varepsilon 2 \mathscr{F}_c Y_2(\mathscr{F}_c) \tag{B9}$$

The first curve is the principal trajectories in the interaction space (g_s, g_c, δ), which joins the fixed points on the $g_c = 0$ plane $[P_{XY}, D_{XY}]$ with those on the $g_c = -\hat{\alpha} g_s$ plane $[P_{XY}^c, D_{XY}^c]$. All the principal trajectories in the region of $-\hat{\alpha} < g_c/g_s < 0$ are contained. The second curve corresponds to the rest of the principal trajectories connecting their fixed points with those on the $g_s = 0$ plane $[P_I, D_I]$.

REFERENCES

1. R. Balian, M. Kleman, and J. Poirier, *Physics of Defects, Les Houches, Session XXXV, 1980* (North-Holland, Amsterdam, 1981); M. Kleman, *Points, Lines and Walls* (John Wiley & Sons, Chichester, 1983).
2. H. Trebin, *Adv. Phys.* **31**:195 (1982); N. D. Mermin, *Rev. Mod. Phys.*, **51C**:591 (1979).
3. A. B. Harris, *J. Phys. C: Sold State* 7:1671 (1974).
4. G. Grinstein and A. Luther, *Phys. Rev. B* **13**:1329 (1976).
5. T. C. Lubensky, *Phys. Rev. B* **11**:3573 (1975).
6. A. Aharony, *Phase Transition and Critical Phenomena*, Vol. VI, C. Domb and M. S. Green, eds. (Academic, New York, 1976).
7. Y. Yamazaki, *Can. J. Phys.* **56**:139 (1978).
8. D. E. Khmel'nitsukii, *Sov. Phys. JETP* **41**:981 (1975).
9. B. N. Shalaev, *Sov. Phys. JETP* **46**:1204 (1978).
10. S. N. Dorogovtsev, *Sov. Phys. Solid State* **22**:188, 1329 (1980).
11. D. Boyanovsky and J. L. Cardy, *Phys. Rev. B* **26**:154 (1982).
12. I. D. Lawrie and V. V. Prudnikov, *J. Phys. C: Solid State* **17**:1655 (1984).
13. A. A. Abrikosov, L. P. Gorkov, and I. E. Dzyaloshinskii, *Quantum Field Theoretical Methods in Statistical Physics* (Pergamon, New York, 1965).

14. B. I. Halperin, P. C. Hohenberg, and S. Ma, *Phys. Rev. B* **10**:139 (1974).
15. P. C. Martin, E. D. Siggia, and H. A. Rose, *Phys. Rev. A* **8**:423 (1973).
16. R. Bausch, H. K. Janssen, and H. Wagner, *Z. Phys. B* **24**:113 (1976).
17. C. de Dominicis and L. Peliti, *Phys. Rev. B* **18**:353 (1978).
18. Y. Yamazaki, *Prog. Theor. Phys.* **55**:1733 (1976).
19. G. t'Hooft and M. Veltman, *Nucl. Phys. B* **44**:185 (1973).
20. J. C. LeGuillou and J. Zinn-Justin, *Phys. Rev. B* **21**:3976 (1980).
21. J. Rudnick, *Phys. Rev. B* **18**:1406 (1978).
22. E. K. Riedel, *Phys. Rev. Lett.* **28**:675 (1972); F. J. Wegner, *Phys. Rev. B* **5**:4529 (1972).
23. L. P. Kadanoff, W. Götze, D. Hamblen, R. Hecht, E. A. S. Lewis, V. V. Palciauskas, M. Ragl, J. Swift, D. Aspnens, and J. Kane, *Rev. Mod. Phys.* **39**:395 (1967).
24. B. I. Halperin, T. C. Lubensky, and S. Ma, *Phys. Rev. Lett.* **32**:292 (1974).
25. S. Coleman and E. Weinberg, *Phys. Rev. D* **7**:1888 (1973).
26. I. D. Lawrie, *Nucl. Phys.* **B200:FS4**, 1 (1982).
27. D. Boyanovsky and J. L. Cardy, *Phys. Rev.* **B25**:7058 (1982).